

100 Years of General Relativity

George F R Ellis
Mathematics Department, University of Cape Town

February 27, 2022

Contents

1	The study of dynamic geometry	3
1.1	Technical developments	3
1.2	Exact Theorems and Global Structure	7
1.3	Singularity theorems	9
1.4	Conclusion	9
2	The Schwarzschild solution and the solar system	10
2.1	The Schwarzschild exterior solution	10
2.2	Effects on particles	11
2.3	Solar system tests of general relativity	11
2.4	Reissner-Nordström, Kottler, and Kerr Solutions	11
2.5	Maximal Extension of the Schwarzschild solution	12
2.6	Conclusion	14
3	Gravitational collapse and black holes	15
3.1	Spherically symmetric matter models	15
3.2	Causal diagrams	15
3.3	Accretion discs and Domains	17
3.4	Powerhouses in astrophysics	17
3.5	Conclusion	17
4	Cosmology and structure formation	18
4.1	FLRW models and the Hot Big Bang	18
4.2	More general dynamics: Inflation	21
4.3	Perturbed FLRW models and the growth of structure	21
4.4	Precision cosmology: Cosmological success and puzzles	22
4.5	More General Geometries: LTB and Bianchi Models	22
4.6	Cosmological success and puzzles	23
5	Gravitational Lensing and Dark Matter	23
5.1	Calculating lensing	24
5.2	Strong lensing	25
5.3	Weak lensing	25
5.4	Microlensing	25
5.5	Conclusion	25

6	Gravitational Waves	26
6.1	Weak field formulation	26
6.2	Exact Gravitational waves	27
6.3	Asymptotic flatness and gravitational radiation	27
6.4	Emission	27
6.5	Gravitational wave detection	28
6.6	Conclusion	29
7	Generalisations	29

Abstract

This is Chapter 1 in General Relativity and Gravitation: A Centennial Perspective, Edited by Abhay Ashtekar (Editor in Chief), Beverly Berger, James Isenberg, Malcolm MacCallum. Publisher: Cambridge University Press (June, 2015). It gives a survey of themes that have been developed during the 100 years of development of general relativity theory.

This chapter aims to provide a broad historical overview of the major developments in General Relativity Theory ('GR') after the theory had been developed in its final form. It will not relate the well-documented story of the discovery of the theory by Albert Einstein, but rather will consider the spectacular growth of the subject as it developed into a mainstream branch of physics, high energy astrophysics, and cosmology. Literally hundreds of exact solutions of the full non-linear field equations are now known, despite their complexity [1]. The most important ones are the Schwarzschild and Kerr solutions, determining the geometry of the solar system and of black holes (Section 2), and the Friedmann-Lemaître-Robertson-Walker solutions, which are basic to cosmology (Section 4). Perturbations of these solutions make them the key to astrophysical applications.

Rather than tracing a historical story, this chapter is structured in terms of key themes in the study and application of GR:

1. The study of dynamic geometry (Section 1) through development of various technical tools, in particular the introduction of global methods, resulting in global existence and uniqueness theorems and singularity theorems.
2. The study of the vacuum Schwarzschild solution and its application to the Solar system (Section 2), giving very accurate tests of general relativity, and underlying the crucial role of GR in the accuracy of useful GPS systems.
3. The understanding of gravitational collapse and the nature of Black Holes (Section 3), with major applications in astrophysics, in particular as regards quasi-stellar objects and active galactic nuclei.
4. The development of cosmological models (Section 4), providing the basis for our understandings of both the origin and evolution of the universe as a whole, and of structure formation within it;
5. The study of gravitational lensing and its astronomical applications, including detection of dark matter (Section 5).
6. Theoretical studies of gravitational waves, in particular resulting in major developments in numerical relativity (Section 6), and with development of gravitational wave observatories that have the potential to become an essential tool in precision cosmology.

This Chapter will not discuss quantum gravity, covered in Part Four. It is of course impossible to refer to all relevant literature. I have attempted to give the reader a judicious mix of path-breaking original research articles, and good review articles. Ferreira has recently discussed the historical development at greater length [2].

1 The study of dynamic geometry

This section deals with the study of dynamic geometry through development of various technical tools, in particular the introduction of global methods resulting in global existence and uniqueness theorems and singularity theorems.

General relativity [3, 4, 5, 6, 7] heralded a new form of physical effect: geometry was no longer seen as an eternal fixed entity, but as a dynamic physical variable. Thus geometry became a key player in physics, rather than being a fixed background for all that occurs. Accompanying this was the radical idea that there was no gravitational force, rather that matter curves spacetime, and the paths of freely moving particles are geodesics determined by the spacetime. This concept of geometry as dynamically determined by its matter content necessarily leads to the non-linearity of both the equations and the physics. This results in the need for new methods of study of these solutions; standard physics methods based on the assumption of linearity will not work in general.

Tensor calculus is a key tool in general relativity [8, 9]. The **space-time geometry** is represented on some specific averaging scale and determined by the **metric** $g_{ab}(x^\mu)$. The curvature tensor R_{abcd} is given by the Ricci identities for an arbitrary vector field u^a :

$$u_{b;[cd]} = u^a R_{abcd} \quad (1)$$

where square brackets denote the skew part on the relevant indices, and a semi-colon the covariant derivative. The curvature tensor plays a key role in gravitation through its contractions, the Ricci tensor $R_{ab} := R^c_{acb}$ and Ricci scalar $R := R^a_a$. The **matter** present determines the geometry, through **Einstein's relativistic gravitational field equations** ('EFE') [3] given by

$$G_{ab} \equiv R_{ab} - \frac{1}{2} R g_{ab} = \kappa T_{ab} - \Lambda g_{ab} . \quad (2)$$

Geometry in turn determines the motion of the matter because the **twice-contracted Bianchi identities** guarantee the conservation of total energy-momentum:

$$\nabla_b G^{ab} = 0 \quad \Rightarrow \quad \nabla_b T^{ab} = 0 , \quad (3)$$

provided the **cosmological constant** Λ satisfies the relation $\nabla_a \Lambda = 0$, i.e., it is constant in time and space. In conjunction with suitable equations of state for the matter, represented by the stress-energy tensor T_{ab} , equations (2) determine the combined dynamical evolution of the model and the matter in it, with (3) acting as integrability conditions.

1.1 Technical developments

Because of the non-Euclidean geometry, coordinate freedom is a major feature of the theory, leading to the desirability of using covariant equations that are true in all coordinate systems if they are true in one. Because of the non-linear nature of the field equations, it is desirable to use exact methods and obtain exact solutions as far as possible, in order to not miss phenomena that cannot be investigated through linearized versions of the equations. A series of technical developments facilitated study of these non-linear equations.

1.1.1 Coordinate free methods and general bases

The first was the use of coordinate free methods, representing vector fields as differential operators, and generic bases rather than just coordinate bases. Thus one notes the differential geometry idea that tangent vectors are best thought of as operators acting on functions [5, 10], thus $X = X^i \frac{\partial}{\partial x^i} \Rightarrow X(f) = X^i \frac{\partial f}{\partial x^i}$, with a coordinate basis $e_i = \frac{\partial}{\partial x^i}$. Then a generic basis e_a ($a = 0, 1, 2, 3$) is given by

$$e_a = \Lambda_a^i(x^j) e_i = \Lambda_a^i(x^j) \frac{\partial}{\partial x^i}, \quad |\Lambda_a^i| \neq 0.$$

There are three important aspects of any basis. First, the commutator coefficients $\gamma_{bc}^a(x^c)$ defined by

$$\gamma_{bc}^a e_a = [e_b, e_c], \quad [X, Y] := XY - YX.$$

The basis e_a is a coordinate basis iff¹ $\gamma_{bc}^a = 0$. Second, the metric components g_{ab} are defined by

$$g_{ab} := e_a \cdot e_b = \Lambda_a^i \Lambda_b^j g_{ij}$$

with inverses g^{ab} determined by $g^{ab}g_{bc} = \delta_c^a$. Indices are raised and lowered by g_{ab} and g^{bc} . The basis is a *tetrad* basis if the g_{ab} are constants. The two key forms of tetrad are null tetrads with two real null vectors and two complex ones, used for studying gravitational radiation, where

$$g_{ab} = \begin{pmatrix} 0 & -1 & 0 & 0 \\ -1 & 0 & 0 & 0 \\ 0 & 0 & 0 & 1 \\ 0 & 0 & 1 & 0 \end{pmatrix},$$

and orthonormal tetrads, used for studying fluid properties, where

$$g_{ab} = \begin{pmatrix} -1 & 0 & 0 & 0 \\ 0 & 1 & 0 & 0 \\ 0 & 0 & 1 & 0 \\ 0 & 0 & 0 & 1 \end{pmatrix}.$$

Third, there are the rotation coefficients Γ_{bc}^a characterizing the covariant derivatives of the basis vectors, defined by

$$\nabla_b e_c = \Gamma_{bc}^a e_a.$$

Using the standard assumptions of (1) metricity: writing $f_{,i} = \frac{\partial f}{\partial x^i}$ this is

$$\nabla_e g_{dc} = 0 \iff g_{dc,e} = \Gamma_{dec} + \Gamma_{ced}$$

and (2) vanishing torsion: writing $f_{;ab} := (f_{;a})_{;b}$, this is

$$f_{;ab} = f_{;ba} \quad \forall f(x^i) \iff \gamma_{ab}^c = \Gamma_{ab}^c - \Gamma_{ba}^c$$

one obtains (3) the generalized Christoffel relations

$$\Gamma_{ced} = \frac{1}{2} (g_{cd,e} + g_{ec,d} - g_{de,c}) + \frac{1}{2} (\gamma_{edc} + \gamma_{dec} - \gamma_{ced}).$$

The first term vanishes for a tetrad, and the second for a coordinate basis. Tetrad bases were used in obtaining solutions by Levi-Civita in the 1920s. Null tetrads were the basis of the Newman-Penrose formalism used primarily to study gravitational radiation [11]; they are closely related to spinorial variables [11]. Orthonormal tetrads have been used to study fluid models and Bianchi spacetimes [12, 13]. Dual 1-form relations, using exterior derivatives, have been used by many workers (e.g. Bel, Debever, Misner, Kerr) to find exact solutions.

1.1.2 Tensor symmetries and the volume element

Second was a realization of the importance of tensor symmetries, for example separating a tensor T_{ab} into its symmetric and skew symmetric parts, and then separating the former into its trace and trace-free parts:

$$T_{ab} = T_{[ab]} + T_{(ab)}, \quad T_{(ab)} = T_{<ab>} + \frac{1}{4} T g_{ab}, \quad T_{<ab>} g^{ab} = 0$$

¹iff means “if and only if”

where $T_{[ab]} = \frac{1}{2}(T_{ab} - T_{ba})$, $T_{(ab)} = \frac{1}{2}(T_{ab} + T_{ba})$, $T = T_{ab}g^{ab}$. This breaks the tensor T_{ab} up into parts with different physical meanings. A tensor equation implies equality of each part with the same symmetry, for example

$$T_{ab} = W_{ab} \Leftrightarrow (T_{[ab]} = W_{[ab]}, T_{<ab>} = W_{<ab>}, T = W).$$

This plays an important role in many studies. Similar decompositions occur for more indices, for example $T_{[abc]} = \frac{1}{6}(T_{abc} + T_{bca} + T_{cab} - T_{acb} - T_{bac} - T_{cba})$. An example is the curvature tensor symmetries

$$R_{abcd} = R_{[ab][cd]} = R_{cdab}, R_{a[bcd]} = 0.$$

Arbitrarily large symmetric tensors can be split up in a similar way into trace-free parts; this is significant for gravitational radiation studies [14] and kinetic theory, in particular studies of CMB anisotropies [15, 16]. In the case of skew tensors, there is a largest possible skew tensor, namely the volume element $\eta_{abcd} = \eta_{[abcd]}$, which satisfies a key set of identities:

$$\eta_{abcd}\eta^{efgh} = -4!\delta_{[a}^e\delta_b^f\delta_c^g\delta_d^h]$$

and others that follow by contraction. These symmetries characterize invariant subspaces of a tensor product under the action of the linear group and so embody an aspect of group representation theory: how to decompose tensor representations into irreducible parts.

1.1.3 Symmetry groups

Third was the systematization of the use of symmetry groups in studying exact solutions. A symmetry is generated by a Killing vector field ξ , a vector field that drags the metric into itself, and so gives a zero Lie derivative for the metric tensor:

$$L_\xi g_{ab} = 0 \Leftrightarrow \xi_{(a;b)} = 0.$$

Such a vector field satisfies the integrability condition

$$\xi_{a;bc} = R_{abcd}\xi^d$$

showing that a solution is determined by the values $\xi_a|_P$ and $\xi_{a;b}|_P$ at a point P. The set of all Killing vectors form a Lie algebra generating the symmetry group for the spacetime. The isotropy group of a point is generated by the set of Killing vector fields vanishing at that point. Exact solutions can be characterized by the group of symmetries, together with a specification of the dimension and causal character of the surfaces of transitivity of the group [12]. The most important symmetries are when a spacetime is (a) static or stationary, (b) spherically symmetric, or (c) spatially homogeneous.

Killing vectors give integration constants for geodesics: if k^a is a geodesic tangent vector, then $E := \xi_a k^a$ is a constant along the geodesic. They also give conserved vectors from the stress tensor: $J^a = T^{ab}\xi_b$ has vanishing divergence: $J^a_{;a} = 0$.

1.1.4 Congruences of curves and geodesic deviation

Fourth was the study of timelike and null congruences of curves (Synge, Heckmann, Schücking, Ehlers, Kundt, Sachs, Penrose) [17, 18, 19], leading to a realisation of the importance of the geodesic deviation equation (GDE) [20] and its physical meaning in terms of expressing tidal forces and gravitational radiation [21, 22]).

The kinematical properties of null and timelike vector fields are represented by their acceleration a_e , expansion θ , shear σ_{de} , and rotation ω_{de} (which are equivalent to some of the Ricci rotation coefficients for associated tetrads [23, 12]). They characterise the properties of fluid flows (the

timelike case), hence are important in the dynamics of fluids, and of bundles of null geodesics (the null case with $a_e = 0$), and so are important in observations in astronomy and cosmology.

The GDE determines the second rate of change of the deviation vectors for a congruence of geodesics of arbitrary causal character, i.e., their relative acceleration. Consider the normalised tangent vector field V^a for such a congruence, parametrised by an affine parameter v . Then $V^a := \frac{dx^a(v)}{dv}$, $V_a V^a := \epsilon$, $0 = \frac{\delta V^a}{\delta v} = V^b \nabla_b V^a$, where $\epsilon = +1, 0, -1$ if the geodesics are spacelike, null, or timelike, respectively, and we define covariant derivation *along* the geodesics by $\delta T^{a\cdots b\cdots}/\delta v := V^b \nabla_b T^{a\cdots b\cdots}$ for any tensor $T^{a\cdots b\cdots}$. A deviation vector $\eta^a := dx^a(w)/dw$ for the congruence, which can be thought of as linking pairs of neighbouring geodesics in the congruence, commutes with V^a , so

$$L_V \eta = 0 \Leftrightarrow \frac{\delta \eta^a}{\delta v} = \eta^b \nabla_b V^a. \quad (4)$$

It follows that their scalar product is constant along the geodesics: $\frac{\delta(\eta_a V^a)}{\delta v} = 0 \Leftrightarrow (\eta_a V^a) = \text{const}$. To simplify the relevant equations, one can choose them orthogonal: $\eta_a V^a = 0$. The general GDE takes the form

$$\frac{\delta^2 \eta^a}{\delta v^2} = -R^a_{bcd} V^b \eta^c V^d, \quad (5)$$

This shows how spacetime curvature causes focussing or defocussing of geodesics, and is the basic equation for gravitational lensing. The general solution to this second-order differential equation along any geodesic γ will have two arbitrary constants (corresponding to the different congruences of geodesics that might have γ as a member). There is a *first integral* along any geodesic that relates the connecting vectors for two *different* congruences which have one central geodesic curve (with affine parameter v) in common. This is $\eta_{1a} \frac{\delta \eta_2^a}{\delta v} - \eta_{2a} \frac{\delta \eta_1^a}{\delta v} = \text{const}$ and is completely independent of the curvature of the spacetime.

The trace of the geodesic deviation equation for timelike geodesics is the Raychaudhuri equation [24]. In the case of timelike vectors $u^a = dx^a/d\tau$ it is the fundamental equation of gravitational attraction for a fluid flow [18, 25]:

$$\frac{d\theta}{d\tau} = -\frac{1}{3}\theta^2 - 2(\omega^2 - \sigma^2) - \frac{\kappa}{2}(\rho + 3p) + \Lambda - a^b{}_{;b}. \quad (6)$$

In the case of null geodesics $k^a = dx^a/d\lambda$ diverging from a source (so $\varepsilon = 0$, $a_e = 0$, $\omega = 0$) it is the basic equation of gravitational focusing of bundles of light rays [5]:

$$\frac{d\theta}{d\lambda} + \frac{1}{2}\theta^2 + \sigma^2 = -R_{ab} k^a k^b. \quad (7)$$

These equations play a key role in singularity theorems.

1.1.5 The conformal curvature tensor

Fifth was a realisation, following on from this, that one could focus on the full curvature tensor R_{abcd} itself, and not just the Ricci tensor. The curvature tensor R_{abcd} is comprised of the Ricci tensor R_{ab} and the Weyl conformal curvature tensor C_{abcd} , given by

$$C_{abcd} := R_{abcd} + \frac{1}{2}(R_{ac}g_{bd} + R_{bd}g_{ac} - R_{ad}g_{bc} - R_{bc}g_{ad}) - \frac{1}{6}R(g_{ac}g_{bd} - g_{ad}g_{bc}). \quad (8)$$

This has the same symmetries as the curvature tensor but in addition is trace-free: $C^c_{acd} = 0$. The Ricci tensor is determined pointwise by the matter present through the field equations, but the Weyl tensor is not so determined: rather it is fixed by matter elsewhere plus boundary conditions. Its value at any point is determined by the Bianchi identities

$$R_{ab[cd;e]} = 0 \quad (9)$$

which are integrability conditions for the curvature tensor that must always be satisfied. In 4 dimensions this gives both the divergence identities $\nabla^d(R_{cd} - \frac{1}{2}Rg_{cd}) = 0$ for the Ricci tensor, which imply matter conservation (see (3)), and divergence relations for C_{abcd} :

$$\nabla^d C_{abcd} = \nabla_{[a}(-R_{b]c} + \frac{1}{6}Rg_{b]c}). \quad (10)$$

Substituting from the field equations (2), matter tensor derivatives are a source for the divergence of the Weyl tensor. Thus one can think of the Weyl tensor as the free gravitational field (it is not determined by the matter at a point), being generated by matter inhomogeneities and then propagating to convey information on distant gravitating matter to local systems. It will then affect local matter behaviour through the geodesic deviation equation. Thus these are Maxwell-like equations governing tidal forces and gravitational radiation effects [26, 10].

This geometrical and physical significance of the Weyl tensor has led to studies of its algebraic structure (the Petrov Classification) *inter alia* by Petrov [27], Pirani, Ehlers, Kundt, and by Penrose using a spinor formalism [28, 11], and use of the Weyl tensor components as auxiliary variables in studies of exact solutions, gravitational radiation, and cosmology. One can search for vacuum solutions of a particular Petrov type [1], and relate asymptotic power series at large distances to outgoing radiation conditions [19, 23, 11].

1.1.6 Junction Conditions

Sixth, many solutions have different domains with different properties, for example vacuum and fluid-filled. An important question then is how to join two different such domains together without problems arising at the join. Lichnerowicz (using a coordinate choice) and Darmois (using coordinate-free methods) showed how to join domains smoothly together, and Israel [29] showed how to assign properties to shock waves, boundary surfaces, and thin shells that could lead to such junctions with a surface layer occurring. The Darmois–Lichnerowicz case is included as the special situation where there is no surface layer.

1.1.7 Generation techniques

Finally, a set of generation techniques were discovered that generated new exact solutions from old ones, for example fluid solutions from vacuum ones. These are discussed extensively in [1].

1.2 Exact Theorems and Global Structure

The results mentioned so far are local in nature, but there has been a major development of global results also (building on the local methods mentioned above). This is covered in detail in Chapter 9 (‘Global Behavior of Solutions to Einstein’s Equations’).

1.2.1 Global properties and causality

The first requirement is a careful use of coordinate charts as parts of atlases that cover the whole spacetime considered and so avoid coordinate singularities. This enables study of global topology, which may often not be what was first expected, and is closely related to the causal structure of the manifold. It is clear that closed timelike lines can result if a spacetime is closed in the timelike direction, but Gödel showed that closed timelike lines could occur for exact solutions of the field equations for pressure-free matter that are simply connected [30]. This occurs basically because, due to global rotation of the matter, light cones tip over as one moves further from the origin. This paper led to an intensive study of causation in curved spacetimes by Penrose, Carter, Geroch, Hawking, and others. The field equations of classical general relativity do not automatically prevent causality violation: so various causality conditions have been proposed as extra conditions to be imposed in addition to the Einstein equations, the most physically relevant being stable causality (no closed

timelike lines exist even if the spacetime is perturbed) [5]. The global structure of examples such as the Gödel universe and Taub-NUT space were crucial in seeing the kinds of pathologies that can occur.

1.2.2 Conformal diagrams and horizons

Studying the conformal structure of a spacetime is greatly facilitated by using conformal diagrams. Penrose pioneered this method [31] and showed that one can rescale the conformal coordinates so that the boundary of spacetime at infinite distance is represented at a finite coordinate value, hence one can represent the entire spacetime and its boundary in this way [31]. For example Minkowski space has null infinities I_- and I_+ for incoming and outgoing null geodesics, an infinity i_0 for spacelike geodesics, and past and future infinities i_- , i_+ for timelike geodesics, and, perhaps surprisingly, the points i_0 , i_- and i_+ have to be identified. Penrose diagrams are now a standard tool in general relativity studies, particularly in cosmology, where they make the structure of particle horizons and visual horizons very clear, and in studying black holes [32].

In the case of cosmology, there was much confusion about the nature of horizons until Rindler published a seminal paper that clarified the confusion [33]. Penrose then showed that the nature of particle horizons could be well understood by characterising the initial singularity in cosmology as spacelike [31]. Nowadays they are widely used in studying inflationary cosmology (but papers on inflation often call the Hubble radius the horizon, when it is not; the particle horizon is non-locally defined). The key feature of black holes is event horizons, which are null surfaces bounding the regions that can send information to infinity from those which cannot; they occur when the future singularity is spacelike. In the case of non-rotating black holes, their nature and relation to the various spacetime domains (inside and outside the event horizon), the existence of two spacelike singularities, and two separate asymptotically flat exterior regions, is fully clarified by the associated Penrose diagrams (Section 3). Carter developed the much more complex such diagrams for the Reissner-Nordstrom charged solution and the Kerr rotating black hole solution [5]. Without these diagrams, it would be very hard indeed to understand their global structure.

1.2.3 Initial data, existence and uniqueness theorems

Provided there are no closed timelike lines, existence of suitable initial data on a spacelike surface S satisfying the initial value equations [34], together with suitable equations of state for whatever matter may be present, determines a unique solution for the Einstein equations within the future domain of dependence of S : that is, the region of spacetime such that all past timelike and null curves intersect S . Applied to the gravitational equations, the spacetime developing from the initial data is called the future Cauchy development of the data on S [5, 35]. An important technical point is that one can prove existence of timelike and null geodesics from S to every point in this domain of dependence. The spacetime is called globally hyperbolic if the future and past domains of dependence cover the entire spacetime; then data on S determines the complete spacetime structure, and S is called a Cauchy surface for the spacetime.

Arnowitt, Deser, and Misner [36] developed the ADM (Hamiltonian based) formalism showing precisely what initial data was needed on S , and what constraint equations it had to satisfy, in order that the spacetime development from that data would be well defined. The initial value problem is to determine what initial data satisfies these constraints. They also formulated the evolution equations needed to determine the time development of this data. Lichnerowicz, Choquet-Bruhat, and Geroch showed existence and uniqueness of a maximal Cauchy development can be proved using functional analysis techniques based on Sobolev spaces. These existence and uniqueness theorems are discussed in Chapter 8.

The study of asymptotically flat spacetimes leads to positive mass theorems. Associated with these theorems are non-linear stability results for the lowest energy solutions of Einstein's equations [the Minkowski and de Sitter space-times] that are discussed in Chapter 9.

1.3 Singularity theorems

Singularities - an edge to spacetime - occur in the Schwarzschild solution and in the standard FLRW models of cosmology. A key issue is whether these are a result of the high symmetry of these spacetimes, and so they might disappear in more realistic models of this situations. Many attempts to prove theorems in this regard by direct analysis of the field equations and examination of exact solutions failed. The situation was totally transformed by a highly innovative paper by Roger Penrose in 1965 [37] that used global methods and causal analysis to prove that singularities will occur in gravitational collapse situations where closed trapped surfaces occur, a causality condition is satisfied, and suitable energy conditions are satisfied by the matter and fields present. A closed trapped surface occurs when the gravitational field is so strong that outgoing null rays from a 2-sphere converge - which occurs inside $r = 2m$ in the Schwarzschild solution. There are various positive energy conditions that play a key role in these theorems, for example the null energy condition $\rho + p \geq 0$, where ρ is the energy density of the matter and p its pressure [5]. Instead of characterising a singularity by divergence of a scalar field such as the energy density, it was characterized in this theorem by geodesic incompleteness: that is, some timelike or null geodesics could not be extended to infinite affine parameter values, showing there is an edge to spacetime that can be reached in a finite time by freely moving particles or photons. Thus their possible future or past is finite. Penrose's paper proved that the occurrence of black hole singularities is not due to special symmetries, but is generic.

This paper opened up entirely new methods of analysis and showed their utility in key questions. Its methods were extended by Hawking, Geroch, Misner, Tipler, and others; in particular Hawking proved similar theorems for cosmology, in effect using the fact that time-reversed closed trapped surfaces occur in realistic cosmological models; indeed their existence can be shown to be a consequence of the existence of the cosmic microwave blackbody radiation [5]. A unifying singularity theorem was proved by Hawking and Penrose [38]. The nature of energy conditions and the kinds of singularities that might exist were explored, leading to characterization of various classes of singularities (scalar, non-scalar, and locally regular), and alternative proposals for defining singularities were given particularly by Schmidt.

1.3.1 A 'major crisis for physics'

John Wheeler emphasized that existence of spacetime singularities - an edge to spacetime, where not just space, time, and matter cease to exist, but even the laws of physics themselves no longer apply - is a major crisis for physics:

The existence of spacetime singularities represents an end to the principle of sufficient causation and to so the predictability gained by science. How could physics lead to a violation of itself - to no physics? [39]

This is of course a prediction of the classical theory. It is still not known if quantum gravity solves this issue or not.

1.4 Conclusion

Because GR moves spacetime from being a fixed geometrical background arena within which physics takes place to being a spacetime that is a dynamical participant in physics, and replaces Euclid's Parallel Postulate by the geodesic deviation equation, it radically changes our understanding of the nature of space-time geometry. Because it conceives of gravity and inertia as being locally indistinguishable from each other, it radically changes our view of the nature of the gravitational force. The resulting theory has been tested to exquisite precision [40, 41]; see also Chapter 2.. Because the curvature of spacetime allows quite different global properties than in flat spacetime, it

is possible for closed timelike lines to occur. Because it allows for a beginning and end to spacetime, where not just matter but even spacetime and the laws of physics cease to exist, it radically alters our views on the nature of existence. What it does not do is give any account of how spacetime might have come into existence: that is beyond its scope.

2 The Schwarzschild solution and the solar system

Karl Schwarzschild developed his vacuum solution of the Einstein equations in late 1915, even before the General Theory of Relativity was fully developed [42]. This is one of the most important solutions in general relativity because of its application to the Solar system (this section), giving very accurate tests of general relativity, because of the remarkable properties of its maximal analytic extension, and because of its application to black hole theory (next sections).

2.1 The Schwarzschild exterior solution

Consider a vacuum, spherically symmetric solution of the Einstein Field Equations. To model the exterior field of the sun in the solar system, or of any static star, we look for a solution that is

(1) spherically symmetric (here we ignore the rotation of the sun and its consequent oblateness, leading to a slightly non-spherical exterior field, as well as the small perturbations due to the gravitational fields of the planets),

(2) vacuum outside some radius r_S representing the surface of a central star or other massive object. Thus we consider the *exterior solution*: $R_{bf} = 0$, ignoring the gravitational field of dust particles, the solar wind, planets, comets, etc. It can be attached at r_S to a corresponding interior solution for the star that generates the field, for example the Schwarzschild interior solution [4] which has constant density (but does not have a realistic equation of state).

We can choose coordinates for which the metric form is manifestly spherically symmetric:

$$ds^2 = -A(r, t)dt^2 + B(r, t)dr^2 + r^2(d\theta^2 + \sin^2\theta d\phi^2) \quad (11)$$

where $x^0 = t$, $x^1 = r$, $x^2 = \theta$, $x^3 = \phi$ (the symmetry group $SO(3)$ acts on the 2-spheres $\{r = \text{const}, t = \text{const}\}$). A major result is the *Jensen-Birkhoff theorem*: the solution necessarily has an extra symmetry (there is a further Killing vector) and so is necessarily static in the exterior region: $A = A(r)$, $B = B(r)$, independent of the time coordinate t [4, 5]. This is a local result: provided the solution is spherically symmetric, it does not depend on boundary conditions at infinity. It implies that spherical objects cannot radiate away their mass (that is, there is no dilaton in general relativity theory). Define $m \equiv MG/c^2 > 0$ (mass in geometrical units, giving the one essential constant of the solution); then, setting $c = 1$,

$$ds^2 = -\left(1 - \frac{2m}{r}\right)dt^2 + \left(1 - \frac{2m}{r}\right)^{-1}dr^2 + r^2(d\theta^2 + \sin^2\theta d\phi^2) \quad (12)$$

This is the Schwarzschild (Exterior) solution [43]. It is an *exact* solution of the EFE (no linearization was involved) for the exterior field of a central massive object. It is valid for $r > r_S$ where r_S is the coordinate radius of the surface of the object; we require that $r_S > r_G \equiv 2m \equiv 2MG/c^2$ where r_G is the gravitational radius or *Schwarzschild radius* of the object; this is the mass in geometrical units. If $r_S < r_G$, we would have a black hole and the interior/exterior matching would be impossible.

It is *asymptotically flat*: as $r \rightarrow \infty$, (12) becomes the metric of Minkowski spacetime in spherically symmetric coordinates. Note that we did not have to put this in as an extra condition: it automatically arose as a property of the exact solution.

2.2 Effects on particles

The spacetime geometry determines how particles move in the spacetime.

2.2.1 Particle Orbits and Light rays

The importance of this solution is that it determines the paths of particles and light rays in the vicinity of the Sun. To determine them one needs to solve the geodesic equations for timelike and lightlike curves. The Lagrangian for geodesics is $L = g_{ab}(x^c)\dot{x}^a\dot{x}^b$ where $\dot{x}^a = dx^a/dv$, with v an affine parameter along the geodesics. Applying this to timelike paths, one determines orbits for planets around the Sun, obtaining standard bound and unbound planetary orbits but with perihelion precession, as confirmed by observations [4]; applying it to photon orbits, one gets equations both for gravitational redshift and for gravitational lensing, again as confirmed by observations [4].

Putting them together, one gets the predictions for laser ranging experiments that have confirmed the predictions of general relativity theory with exquisite precision [40]. One can also determine the proper time measured along any world line and combine it with the gravitational redshift and Doppler shift predictions for signals from a satellite to Earth, thereby providing the basis for precision GPS systems [44]. Thus GR plays a crucial role in the accuracy of useful GPS systems.

2.2.2 Spin precession

Parallel transport along a curve corresponds to Fermi-Walker transport along the curve, leading to the prediction of spin precession, or frame dragging. This can be measured by gyroscope experiments, as tested recently by gravity probe B [45]. The effect is also observable in binary pulsars [46].

2.3 Solar system tests of general relativity

This set of results enables precision tests of General Relativity in the Solar Systems. Clifford Will and others have set up a Parameterized Post-Newtonian (PPN) formalism [40]. whereby general relativity can be compared to other gravitational theories through this set of experiments, that is 1. Planetary orbits; 2. Light bending; 3. Radar ranging; 4. Frame Dragging experiment; 5. Validation of GPS systems. These solar system tests of GR establish its validity on solar system scales to great accuracy. They are discussed in detail in Chapter 2.

Together these tests confirm that Einstein's gravitational theory - a radical revolution in terms of viewing how gravitation works, developed by pure thought from careful analysis of the implications of the equivalence principle - is verified to extremely high accuracy. There is no experimental evidence that it is wrong.

2.4 Reissner-Nordström, Kottler, and Kerr Solutions

There are three important generalizations of the Schwarzschild solution.

2.4.1 Reissner-Nordström solution

Firstly, there is the Reissner-Nordström solution, which is the charged version of the Schwarzschild solution [47, 48], where in (11) the factor $A(r, t) = 1 - \frac{2m}{r} + \frac{GQ^2}{\epsilon r^2} = 1/B(r, t)$. It is spherically symmetric and static, but has a non-zero electric field due to a charge Q at the centre. It is of considerable theoretical interest, but is not useful in astrophysics, as stars are not charged (if they were, electromagnetism rather than gravitation would dominate astronomy).

2.4.2 Kottler solution

Secondly, the generalization of this spacetime to include a cosmological constant Λ is the Kottler solution [49], where in (11) the factor $A(r, t) = 1 - \frac{2m}{r} - \frac{\Lambda r^2}{3} = 1/B(r, t)$, which is a Schwarzschild solution with cosmological constant. It gives the field of a spherical body imbedded in a de Sitter universe. This is relevant to the present day universe, because astronomical observations have detected the effect of an effective cosmological constant in cosmology at recent times.

2.4.3 Kerr solution

Finally there is the Kerr solution [50, 51] which is the rotating version of the Schwarzschild solution. It is a vacuum solution that is stationary rather than static and axially symmetric rather than spherically symmetric [4, 5]. It is of considerable importance because most astrophysical objects are rotating. There is one important difference from Schwarzschild: while we can construct exact interior solutions to match the Schwarzschild exterior solution, that is not the case for the Kerr solution. It has a complex and fascinating structure that is still giving new insights [52].

The geodesic structure of these spaces can be examined as in the case of the Schwarzschild solution. Carter showed that in the case of the Kerr solution, there were hidden integrals for geodesics associated with existence of Killing tensors [53, 54].

2.5 Maximal Extension of the Schwarzschild solution

The previous section considered the solution exterior to the surface of a star, and this was all known and understood early on, certainly by the mid 1930s. The behaviour at the coordinate singularity at $r = 2m$ is another matter: despite useful contributions by Eddington, Finkelstein, Szekeres, and Synge, it was only fully understood in the late 1960s through papers by Kruskal and Fronsdal (see [55, 56] for the early historical development).

Consider now the Schwarzschild solution as a vacuum solution with no central star. It is then apparently singular at $r = 2m$, so has to be restricted to $r > 2m$; then both ingoing and outgoing null geodesics are incomplete, because they cannot be extended beyond $r = 2m$. However the scalar invariant $R_{abcd} R^{abcd} = \frac{48m^2}{r^6}$ is finite there, and it turned out this is just a coordinate singularity: one can find regular coordinates that extend the solution across this surface, which is in fact a null surface where the solution changes from being static but spatially inhomogeneous (for $r > 2m$) to being spatially homogeneous but time varying (for $0 \leq r < 2m$).

Eddington, Szekeres, Finkelstein, and Novikov showed how one could find regular coordinates that cross the surface $r = 2m$. To do so, one can note that radial null geodesics are given by $\frac{dt}{dr} = \pm \frac{1}{1 - \frac{2m}{r}} \Leftrightarrow t = \pm r^* + \text{const}$ where $dr^* = \frac{dr}{1 - \frac{2m}{r}} \Leftrightarrow r^* = r + 2m \ln \left(\frac{r}{2m} - 1 \right)$. Defining $v = t + r^*$, $w = t - r^*$, one can obtain three null forms for the Schwarzschild metric. Changing to coordinates (v, r, θ, ϕ) , the metric is

$$ds^2 = -\left(1 - \frac{2m}{r}\right)dv^2 + 2dvdr + r^2 d\Omega^2 \quad (13)$$

which is the Eddington-Finkelstein form of the metric [57]. The coordinate transformation has succeeded in getting rid of the singularity at $r = 2m$, and shows how infalling null geodesics can cross from $r > 2m$ to $r < 2m$, but the converse is not possible, as can be seen in the Eddington-Finkelstein diagram (Figure 1), which shows how the light cones tip over at different radii. This is thus a *black hole* because light cannot escape from the interior region $r < 2m$ to the exterior region $r > 2m$. The coordinate surfaces $\{r = \text{const}\}$ are timelike for $r > 2m$, null for $r = 2m$, and spacelike for $r < 2m$; the coordinate surfaces $\{t = \text{const}\}$ are spacelike for $r > 2m$, undefined for $r = 2m$, and timelike for $r < 2m$. This warns us not to expect that a coordinate t will necessarily be a good time coordinate everywhere just because we call it "time".

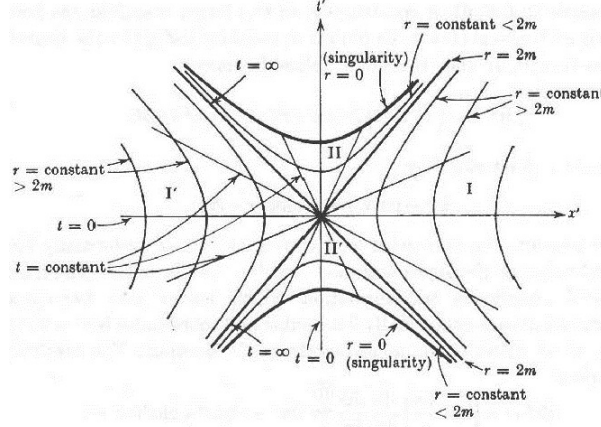


Figure 2. The Kruskal maximal extension of the Schwarzschild vacuum solution.

The singularities are spacelike boundaries to spacetime (one in the future and one in the past), not timelike world lines as one would expect. The coordinate singularities in the original Schwarzschild form of the metric are because the time coordinate t diverges there. Use of conformal transformations of the null coordinates yields the Penrose diagram of the maximally extended spacetime including its boundaries at infinity [5, 4].

2.5.1 Symmetries

The solution is invariant under

- (a) A left-right symmetry, where regions I and I' are identical to each other, while regions II and II' are individually symmetric under the interchange $t' \rightarrow -t'$;
- (b) A time symmetry, where regions II and II' are identical to each other, while regions I and I' are individually symmetric under the interchange $x' \rightarrow -x'$;
- (c) The boost symmetry that is shown to exist by Birkhoff's theorem, with timelike orbits in regions I and I', spacelike orbits in regions II and II', and null orbits in the four null horizons (Killing vector orbits) that bifurcate at the central 2-sphere, which is a set of fixed points of the group. This saddle-point behaviour is a generic property of bifurcate Killing horizons, where the affine parameter and Killing vector parameter are exponentially related to each other [59].

2.5.2 Reissner-Nordström, Kottler, and Kerr Solutions

As shown by Carter [60] and Boyer and Lindquist [61], one can obtain similar maximal extensions of the Reissner-Nordström and Kerr solutions [60, 5]. They are far more complex than those for the Schwarzschild solution, having many horizons and asymptotically flat regions. Lake and Roeder have given the maximal extension for the Kottler spacetime [62].

2.6 Conclusion

The Schwarzschild solution enables us to model the geometry of the solar system with exquisite precision, giving a more accurate description of solar system dynamics than Newtonian theory does. This enables us to test the static aspects of general relativity to very high accuracy, and so confirm its correctness as one of the fundamental theories of physics.

The maximally extended Schwarzschild solution is an extraordinary discovery. The very simple looking metric (12) implies the existence of two asymptotically flat spacetime regions connected by

a wormhole; event horizons (the null surfaces $r = 2m$) separating the interior ($r < 2m$) and exterior ($r > 2m$) regions; and two singularities that are spatially homogeneous in the limit $r \rightarrow 0$. It is impossible for a maximally extended solution to be static. There is no central worldline, as a point particle picture suggests. Thus just as quantum physics implied a radical revision of the idea of a particle, so does general relativity: there is no general relativity version of the Newtonian idea of a point particle.

None of this is obvious. The global topology is not optional; it follows from the way the Einstein equations for this vacuum curve spacetime. And the nature of this solution emphasizes why one should always try to determine exact properties of solutions in general relativity: the global properties of the linearised form of the Schwarzschild solution (which does not exactly satisfy the field equations) will be radically different.

3 Gravitational collapse and black holes

Astrophysical black holes exist because they arise by the collapse of matter due to its gravitational self-attraction.

3.1 Spherically symmetric matter models

Spherically symmetric fluid filled models enable one to investigate how gravitational attraction makes matter aggregate from small perturbations into major inhomogeneities that enter the non-linear regime and form black holes. Pressure-free models one can use to investigate this are the Lemaître-Tolman-Bondi models [63, 64, 65] which evolve inhomogeneously with spherical shells each obeying a version of the Friedmann equation of cosmology. One can use these as interior solutions, with the Schwarzschild solution as the exterior (vacuum) solution, joined across a timelike surface where the standard junction conditions (Section 1.1.6) are fulfilled. More realistic models with pressure obey the Oppenheimer-Volkov equation of evolution [4]. Astrophysical studies show that if the collapsing object is massive enough (its mass is greater than the Chandrasekhar limit), there is no physical pressure that will halt the collapse: the final state will be a black hole [4, 66]. Using pressure-free models to investigate gravitational collapse, Oppenheimer and Snyder showed this would eventually occur: *"we see that for a fixed value of R as t tends toward infinity, τ tends to a finite limit, which increases with R . After this time τ_0 an observer comoving with the matter would not be able to send a light signal from the star; the cone within which a signal can escape has closed entirely."* [67].

3.2 Causal diagrams

Basically the situation is like Figure 1, but the solution's central part of the diagram is no longer vacuum; it is cut off by the infalling fluid. Initially the surface of the fluid is at $r_S > 2m$ so there are no closed trapped surfaces. Then the fluid surface crosses the value $r_S = 2m$ and thereafter lies inside the event horizon. Light emitted from the surface of the star at later times is trapped behind the event horizon and cannot emerge to the outside world.

The space-time diagram showing how this occurs is given in Figure 3: the event horizon at $r = 2m$ is a null surface, so light emitted at that radius never moves inwards or outwards; the gravitational attraction of the mass at the centre holds it at a constant distance from the centre. From the outside, the collapse never seems to end; there is always light arriving at infinity from just outside the event horizon, albeit with ever increasing redshift and hence ever decreasing intensity.

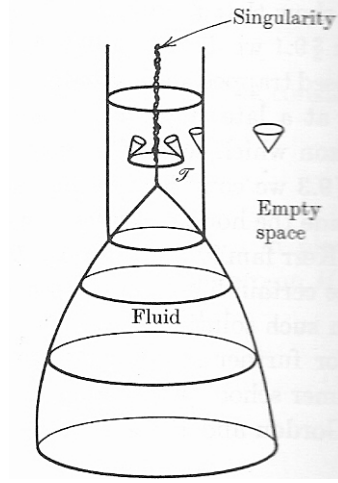


Figure 3. Collapse to a black hole.

However this diagram is misleading in some ways: it suggests that the central singularity is a timelike world line, which is not the case; it is spacelike because it exists in the part of spacetime corresponding to region II in Figure 2. The Penrose diagram for what happens is shown in Figure 4; it shows that the outer regions are the same as region I in Figure 2, but existence of the infalling star leads to a regular centre rather than another asymptotically flat region I' . A key feature, pointed out by Penrose, is that closed trapped surfaces exist for region II given by $r < 2m$: the area spanned by outgoing null geodesics from each 2-sphere decreases as one goes to the future. This is the reason that the occurrence of a singularity in the future is inevitable [37, 39].

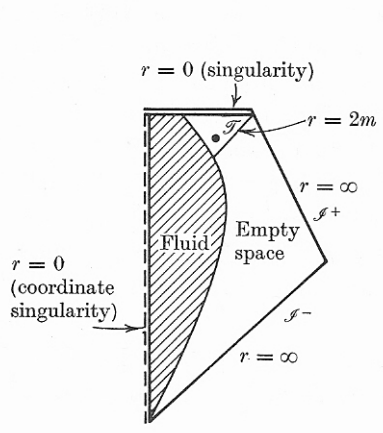


Figure 4. Penrose diagram of collapse to a black hole.

The question then is, how generic is this situation where the final singularity is hidden behind the horizon and so is invisible to the external world: does this only occur in spherically symmetric spacetimes? A very innovative uniqueness theorem by Israel [68] stated that black holes must necessarily be spherically symmetric if a regular event horizon forms. But then the question is, how general is formation of an event horizon? Penrose formulated the cosmic censorship hypothesis, that such horizons would indeed form in the generic case [69]. This conjecture is still unresolved; it is discussed in Chapter 9.

Much effort has been extended in showing that the Kerr solution is the likely final state of gravitational collapse of a rotating object. Work by Hawking, Carter, Robinson and others shows this indeed seems to be the case [70]. Black hole uniqueness theorems are discussed in chapter 9.

An important feature in such collapse is the Penrose inequality relating mass and black hole horizon areas, discussed in Chapter 8, and Hawking's area theorem, which states that the area of cross sections of a black hole horizon is non-decreasing towards the future. This leads to the proposed laws of black hole thermodynamics, associating a temperature and entropy to black holes in a way that is parallel to the usual laws of thermodynamics [71], in particular the temperature is $T_H = \frac{\kappa}{2\pi}$ where κ is the surface gravity of the hole, and the black hole entropy is proportional to the area of its event horizon divided by the Planck area: $S_{BH} = \frac{kA}{4\pi l_P^2}$ where l_P is the Planck length. This led on to Hawking's famous discovery of the emission of black body radiation by black holes through quantum field theory processes; that development however lies outside the scope of this chapter.

3.3 Accretion discs and Domains

Black holes will generally be surrounded by accretion discs that will emit X-rays due to viscous heating as the matter falls in towards the event horizon (see Chapter ??). Rotating black holes have three important domains affecting this process [72]:

1. *The Event Horizon*: That radius inside of which escape from the black hole is not possible;
2. *The Ergosphere*: That radius inside of which negative energy states are possible (giving rise to the potentiality of tapping the energy of the black hole).
3. *Innermost Stable Circular Orbit (ISCO)*: That radius inside of which free circular orbital motion is not possible.

These are the geometric features on which the theory of accretion discs is based.

3.4 Powerhouses in astrophysics

Black holes are intriguing aspects of general relativity, and theoretical studies showed they were indeed likely to form in astrophysical situations. But are they relevant to the universe out there?

It seems indeed so. They were discovered theoretically as an unexpected consequence of the maximal extensions of the Schwarzschild solution. They became central to high energy astrophysics, as shown by Lynden Bell and Rees, being the key to understanding of QSOs [73, 66]. Furthermore supermassive black holes occur in many galaxies, surrounded by accretion disks [74], while stellar mass black holes occur as the endpoint of the lives of massive stars [75]. There is much astronomical evidence for their existence [76] including one at the centre of our own galaxy [77, 78]. The accretion disks that emit radiation whereby we can detect them can be modelled in a general relativity way [72]. This is all discussed in Chapter 3 on relativistic astrophysics, considering the observational status of black holes, and their relation to gamma ray bursts. Chapter 7 discusses how numerical simulations have provided insights into the critical phenomenon at the threshold of black hole formation, gravitational collapse, mergers of black holes, and mergers of black holes and neutron stars.

3.5 Conclusion

Black holes were theoretically predicted to occur because they are solutions of the Einstein Field Equations, but have turned out to play a key role in high energy astrophysics [66]. They occur as the endpoint of evolution of massive stars, and occur at the centre of galaxies, where they play a key role in galaxy dynamics and provide the powerhouse for high energy astrophysical phenomena that are otherwise inexplicable. Furthermore, black hole interactions are expected to provide the source of gravitational waves that will enable us to probe the extremely early universe with great precision

(Section 6.5). They have no analogue in Newtonian gravitational theory because there is no limit to the speed of propagation of signals in that theory (where the speed of light plays no special role).

4 Cosmology and structure formation

The development of cosmological models based in General Relativity theory provides the basis for our understandings of both the evolution of the universe as a whole, and of structure formation within it. The start was Einstein's static universe model of 1917 [79], followed by the static de Sitter universe in 1917, Friedmann's expanding models of 1922 [80] and 1924 [81], and Lemaitre's expanding model of 1927 [82, 83]. These expanding models were ignored until Eddington's proof of the instability of the Einstein static universe in 1930 [84]. The idea of the expanding universe was then generally accepted, and canonised in Robertson's fine review article in 1933 [85] (which gives annotated references to all the earlier papers). It is noteworthy that the first Newtonian cosmological models were developed only in 1935 by Milne and McCrea - some 18 years after the first general relativistic models.

Today the 'standard model of cosmology', based in the way general relativity shows how matter curves spacetime, is highly successful in describing precision observations of the large scale properties of the universe, although some significant problems concerning the nature of the matter and energy fields controlling the dynamics of the universe remain unresolved [86, 87, 10].

4.1 FLRW models and the Hot Big Bang

The expanding universes of Friedmann and Lemaitre ('FL') are a family of exact solutions of the Einstein field equations that are spatially homogenous and isotropic. The geometry of these standard models was clarified by Robertson and Walker ('RW') in 1935. The metric is characterised by a scale factor $a(t)$ representing the time change of the relative size of the universe:

$$ds^2 = -dt^2 + a^2(t)d\sigma^2, \quad d\sigma^2 = dr^2 + f^2(r)d\Omega^2$$

with $f(r) = \{\sin r, r, \sinh r\}$ if $k = \{+1, 0, -1\}$ and $d\Omega^2 = d\theta^2 + \sin^2\theta d\phi^2$; thus the 3-space metric $d\sigma^2$ represents a 3-space of constant curvature k . Spatial homogeneity together with isotropy implies that a multiply transitive group of isometries G_6 acts on the surfaces $\{t = \text{constant}\}$, and consequently all physical and geometric quantities depend only on t . The 4-velocity $u^a = dx^a/dt$ of preferred fundamental observers is

$$u^a = \delta_0^a \Rightarrow u^a u_a = -1$$

so the time parameter t represents proper time measured along fundamental world lines $x^a(t)$ with u^a as tangent vector; the distances between these world lines scales with $a(t)$, so volumes scale as $a^3(t)$. The relative expansion rate of matter is represented by the Hubble parameter $H(t) = (1/a)(da/dt)$, and the rate of slowing down by the deceleration parameter $q := -(1/a)(d^2a/dt^2)$. These space times are conformally flat: $C_{abcd} = 0$ (there is no free gravitational field, so no tidal forces or gravitational waves occur in these models).

4.1.1 Dynamics

The behaviour of matter and expansion of the universe are governed by three related equations. First, the energy conservation equation (3) becomes

$$d\rho/dt + 3H(\rho + p) = 0 \tag{14}$$

relating the rate of change of the energy density $\rho(t)$ to the pressure $p(t)$. It becomes determinate when we are given an equation of state $p = p(\rho, \phi)$ determining p in terms of ρ and possibly some

internal variable ϕ (which if present, will have to have its own dynamical equations). The normalized density parameter is $\Omega := \frac{\kappa\rho}{3H^2}$. The Raychaudhuri equation (6) becomes

$$\frac{3}{a} \frac{d^2 a}{dt^2} = -\frac{\kappa}{2}(\rho + 3p) + \Lambda \quad (15)$$

which directly gives the deceleration due to matter, and shows (i) the active gravitational mass density is $\rho_{grav} := \rho + 3p$, which is positive for all ordinary matter, and (ii) a cosmological constant Λ causes acceleration iff $\Lambda > 0$. Its first integral is the Friedmann equation

$$3H^2 = \kappa\rho + \Lambda - \frac{3k}{a^2}, \quad (16)$$

where $\frac{3k}{a^2}$ is the curvature of the 3-spaces; this is just the Gauss-Codazzi equation relating the curvature of imbedded 3-spaces to the curvature of the imbedding 4-dimensional spacetime [18, 25]. The evolution of $a(t)$ is determined by any two of (14), (15), and (16).

The basic behaviour has been known since the 1930s [85]. Normal matter can be represented by the equation of state $p = (\gamma - 1)\rho$, where $\gamma = 1$ for pressure free matter (‘dust’ or ‘baryonic matter’); $\gamma = 4/3$ for radiation; and $\gamma = -1$ is equivalent to a cosmological constant. There is always a singular start to the universe at time $t_0 < 1/H_0$ ago if $\rho + 3p > 0$, which will be true for ordinary matter plus radiation, and $\Lambda \leq 0$; however one can get a bounce if both $\Lambda > 0$ and $k = +1$ (for matter with $\rho > 0$, bounces can only occur if $k = +1$). When $\Lambda = 0$, if $k = +1$, $\Omega > 1$ the universe recollapses; if $k = -1$, $\Omega < 1$ it expands forever; and $k = 0$ ($\Omega = 1$) is the critical case separating these behaviours, that just succeeds in expanding forever. When $\Lambda > 0$ and $k = +1$, a static solution is possible (the Einstein static universe [88]), and the universe can bounce or ‘hover’ close to a constant radius (these are the Eddington-Lemaître models). All these behaviours can be illuminatingly represented by appropriate dynamical systems phase planes [89, 90].

4.1.2 Observational relations

Observational relations can be worked out for these models, based on the fact that photons move on null geodesics $x^a(v)$ with tangent vector $k^a(v) = dx^a/dv : k^a k_a = 0, k^a_{;b} k^b = 0$ [91]. This shows that the radial coordinate value of radial null geodesics through the origin (which are generic null geodesics, because of the spacetime symmetry) is given by $\{ds^2 = 0, d\theta = 0, d\phi = 0\}$ which gives

$$u(t_0, t_1) := \int_0^{r_{emit}} dr = \int_{t_{emit}}^{t_{obs}} \frac{dt}{a(t)} = \int_{a_{emit}}^{a_{obs}} \frac{1}{H(t)} \frac{da}{a^2(t)}. \quad (17)$$

Substitution from the Friedmann equation (16) shows how the cosmological dynamics affects $u(t_0, t_1)$. Key variables resulting are observed redshifts z , given by

$$1 + z = \frac{(k^a u_a)_{emit}}{(k^b u_b)_{obs}} = \frac{a(t_{obs})}{a(t_{emit})},$$

and area distance r_0 , which up to a redshift factor is the same as the luminosity distance D_L :

$$D_L = r_0(1 + z);$$

this is the reciprocity theorem [92, 25]. One can work out observational relations for galaxy number counts versus magnitude (n, m) and the magnitude–redshift relation (m, z) , which determines the present deceleration parameter q_0 when applied to “standard candles” [93]. A power series derivation of observational relations in generic cosmological models is given by Kristian and Sachs [91].

Major observational programmes have examined these relations and determined H_0 and q_0 , showing that, assuming the geometry is indeed that of a Robertson-Walker spacetime, the universe is accelerating at recent times ($q_0 < 0$). This means some kind of dark energy is present such that at

recent times, $\rho + 3p < 0$ [86, 87, 10]. The simplest interpretation is that this is due to a cosmological constant $\Lambda > 0$ that dominates the recent dynamics of the universe.

A key finding is the existence of limits both to causation, represented by particle horizons, and to observations, represented by visual horizons. The issue is whether $u(t_0, t_1)$ converges or diverges as $t_0 \rightarrow 0$; and for ordinary matter and radiation, it converges, representing a limit to how far causal effects can propagate since the start of the universe. Much confusion about their nature was cleared up by Rindler in a classic paper [33], with further clarity coming from use of Penrose causal diagrams for these models [31]. This showed that particle horizons would occur if and only if the initial singularity was spacelike. There are many statements in the literature that such horizons represent motion of galaxies away from us at the speed of light, but that is not the case; they occur due to the integrated behaviour of light from the start of the universe to the present day [94], with the visual horizon, determined by the most distant matter we can detect by electromagnetic radiation, lying inside the particle horizon. This is why the visual horizon size can be 42 billion light years in an Einstein de Sitter model with a Hubble scale of 14 billion years. Event horizons relate to the ultimate limits of causation in the future universe, that is whether $u(t_0, t_1)$ converges or diverges as $t_1 \rightarrow \infty$; while they play a key role as regards the nature of black holes (Section 2.5), they are irrelevant to observational cosmology.

4.1.3 Cosmological physics

Cosmological models started off as purely geometrical, but then a major realisation was that standard physics could be applied to the properties of matter in the early universe.

First was the application of atomic physics to the expanding universe, resulting in prediction of a Hot Big Bang ('HBB') early phase of the universe with ionised matter and radiation in equilibrium with each other because of tight coupling between electrons and radiation. This phase ended when the temperature dropped below the ionisation temperature of the matter, resulting in cosmic blackbody radiation being emitted at the Last Scattering Surface at about $T_{emit} = 4000K$. A major theoretical result, consequent on the reciprocity theorem, is that the blackbody spectrum will be preserved but with temperature $T_{obs} = T_{emit}/(1+z)$ [25]; hence this radiation is observed today as cosmic microwave blackbody radiation (CMB) with a temperature of $2.73K$. There then follows a complex interaction of matter and radiation in the expanding universe [95, 96]. A key feature is the evolution of the speed of sound with time, as well as diffusion effects leading to damping of fine-scale structure [97].

Second was the application of nuclear physics to the epoch of nucleosynthesis at a temperature of about $T = 10^8K$, leading to predictions of light element abundances resulting from nuclear interactions in the early universe [98, 99, 95]. The key point here is that the Friedmann equation for early times, when radiation dominates the dynamics and curvature is negligible, gives the temperature-time relation [100]

$$T = \frac{T_0}{t^{1/2}}, T_0 := 0.74 \left(\frac{10.75}{g_*} \right)^{1/2} \quad (18)$$

with no free parameters. Here t is time in seconds, T is the temperature in MeV, and g_* is the effective number of particle species, which is 10.75 for the standard model of particle physics, where there are contributions of 2 from photons, $7/2$ from electron-positron pairs and $7/4$ from each neutrino flavor. It is this relation that determines the course of the nuclear reactions, leading to formation of light elements (up to Lithium) in the early universe. These element abundances agree with those determined by astronomical observations, up to some unresolved worries about Lithium. It was this theory that established cosmology as a solid branch of physics [100].

4.1.4 In summary

These models are the opposite of the Schwarzschild vacuum solution. Those models represent the dynamics of pure vacuum (there is no matter tensor); these models represent the dynamics of spacetime governed purely by matter (there is no free gravitational field). Hence the outcome depends irrevocably on the type of matter present, as shown for example in the dependence (18) of $T(t)$ on g_* . They are remarkably simple, and remarkably good models of the real universe we observe by means of astronomical observations. They also represent a key conundrum: they predict a start to the universe, and indeed all of physics, at a spacetime singularity. One key issue is whether that conclusion can somehow be avoided.

4.2 More general dynamics: Inflation

The previous section was based in well established physics. At earlier times more speculative physics will necessarily be involved, involving interactions not yet testable by particle accelerators.

More general matter dynamics will lead to more general behaviour of the cosmological model at early times. In particular a scalar field $\phi(t)$ with potential $V(\phi)$ may be present, obeying the Klein Gordon Equation

$$d^2\phi/dt^2 + 3H\dot{\phi} + dV/d\phi = 0. \quad (19)$$

It will have an energy density $\rho = \frac{1}{2}(\dot{\phi})^2 + V(\phi)$ and pressure $p = \frac{1}{2}(\dot{\phi})^2 - V(\phi)$, so the inertial and gravitational energy densities are

$$\rho + p = (\dot{\phi})^2 > 0, \quad \rho + 3p = (\dot{\phi})^2 - V(\phi). \quad (20)$$

Hence the active gravitational mass can be negative in the ‘slow roll’ case: $(\dot{\phi})^2 < V(\phi)$. So scalar fields can cause an exponential acceleration when ϕ stays at a constant value ϕ_0 because of the friction term $3H\dot{\phi}$ in (19) resulting in $\rho + 3p \approx -V(\phi_0) = \text{const}$. This is the physical basis of the *inflationary universe* idea of an extremely rapid exponential expansion at very early times that smooths out and flattens the universe, also causing any matter or radiation content to die away towards zero. The inflaton field itself dies away at the end of inflation when slow rolling comes to an end and the inflaton gets converted to matter and radiation by a process of reheating.

It is now broadly agreed that there was indeed such a period of inflation in the very early universe but the details are not clear: there are over 100 different variants [101], including single-field inflation, multiple-field inflation, and models where matter is not described by a scalar field as, for example vector inflation. As the potential is not tied in to any specific physical field, one can run the field equations backwards to determine the effective inflaton potential from the desired dynamic behaviour [102, 103].

4.3 Perturbed FLRW models and the growth of structure

The real universe is only approximately a Robertson-Walker spacetime. Structure formation in an expanding universe can be studied by using linearly perturbed FLRW models at early times, plus numerical simulations at later times when the inhomogeneities have gone non-linear [104, 105]. The development of the theory of the present structure formation, a major theoretical achievement, is described illuminatingly by Longair ([97], Chapter 15), which gives full references: it is only possible to highlight a few of these papers in this brief section (and see also Chapter 4 in this volume).

Lemaitre initiated the use of inhomogeneous models to study structure formation [106, 107, 108]. The study of general linear perturbations of an expanding universe was initiated by Lifshitz [109], and the path-breaking paper by Sachs and Wolfe [110] first studied their effect on microwave background radiation anisotropies. That paper was very careful about gauge freedom. However many others were not, being plagued by the gauge problem: because of absence of a fixed background spacetime,

one can encounter unphysical gauge modes that are essentially just coordinate fluctuations. A path-breaking paper by Bardeen [111] developed a gauge covariant approach to linear perturbations that enabled distinguishing of physical from coordinate modes, and this approach [112, 113] is widely used. An alternative 1+3 covariant approach was initiated by Hawking [114] and then developed by Ellis, Bruni, and collaborators [115, 116]. Both methods have been used to study both structure formation and associated CMB anisotropies [86, 117, 10, 87]. The perturbation equations can for example be used to determine the dynamical effects of the cosmological constant [118].

Key aspects of CMB anisotropies are the baryon-acoustic oscillations before decoupling [119, 120, 104], which lead to the observed CMB power spectrum peaks, and the Sunyaev-Zeldovich effect (scattering of the CMB by ionised hot gas in clusters of galaxies) after decoupling [96, 121], which acts as sensitive test of conditions at the time of scattering. The perfection of the calculations by Silk and Wilson [122] and Bond and Efstathiou [123], and the subsequent explosion of precision calculations (as opposed to measurements) in the 90s, based on the growth of fluctuations seeded by quantum fluctuations in the inflationary era [112, 113], is one of the great success stories in cosmology ([97]: Chapter 13). A key realisation was that introduction of a cosmological constant would allow a cold dark matter scenario to match observations of an almost flat universe [124].

4.4 Precision cosmology: Cosmological success and puzzles

Use of the perturbed FLRW models in conjunction with extraordinary observational advances has led to an era of precision cosmology, combining physics and astrophysics with general relativity to predict both the background model evolution plus the growth of structure in it. Key features are: the dynamical evolution of the background model, with an inflationary era followed by a hot big bang era, a matter dominated era, and a dark energy dominated late era; physical modelling of the hot big bang era, including nucleosynthesis and matter-radiation decoupling leading to CMB with a precise black body spectrum; models of galaxy and other source numbers with respect to distance as well as luminosity versus distance relations; modelling of structure formation, related to matter power spectra and Baryon Acoustic Oscillations; and prediction of CMB angular power spectra. Together they comprise the concordance model of cosmology [86, 117, 10, 87].

The puzzles are that we do not know the nature of the inflaton, for which there are over 100 models [101]; we do not know the nature of the dark matter that is indicated to exist by dynamical studies, and is far more abundant than baryonic matter; and we do not know the nature of the dark energy causing an acceleration of the expansion of the universe at late times. It is possible that some of these issues may be indicating we need a different theory of gravity than general relativity, for example MOND or a scalar-tensor theory.

4.5 More General Geometries: LTB and Bianchi Models

There are two other classes of exact solutions that have been used quite widely in cosmological studies.

4.5.1 LTB spherically symmetric models

Firstly, the growth of inhomogeneities may be studied by using exact spherically symmetric solutions, enabling study of non-linear dynamics. The zero pressure such models are the Lemaître-Tolman-Bondi exact solutions [64, 65] where the time evolution of spherically symmetric shells of matter is governed by a radially dependent Friedmann equation. The solutions generically have a matter density that is radially dependent, as well as a spatially varying bang time. These models can be used to study (i) the way a spherical mass with low enough kinetic energy breaks free from the overall cosmic expansion and recollapses, hence putting limits on the rate of growth of inhomogeneities [125], and (ii) the way that any observed (m, z) and (N, z) relations can be obtained in a suitable LTB model where one runs the EFE backwards to determine the free functions in the metric from

observations, for any value whatever of the cosmological constant Λ [126, 10]. This opens up the possibility of doing away with the need for dark energy if we live in an inhomogeneous universe model, where the data usually taken to indicate a change of expansion rate in time due to dark energy are in fact due to a variation of expansion rate in space. However although the supernova observations can be explained in this way, detailed observational studies based in the kinematic Sunyaev-Zeldovich effect show this is unlikely [10].

4.5.2 The Bianchi models and phase planes

Secondly, following the work of Gödel, Taub, and Heckmann and Schüking, there is a large literature examining the properties of spatially homogeneous anisotropically expanding models. These models are generically invariant under 3-dimensional continuous Lie groups of symmetries, whose Lie algebra was first investigated by Luigi Bianchi using projective geometry; much simpler methods are now available [13]. Special cases allow higher symmetries (Locally Rotationally Symmetric models [12]). These allow a rich variety of non-linear behaviour, including anisotropic expansion at early and late times even if the present behaviour is nearly isotropic; different expansion rates at the time of nucleosynthesis than in FLRW models, leading to different primordial element abundances; complex anisotropy patterns in the CMB sky; and much more complex singularity behaviour than in FLRW models, including cigar singularities, pancake singularities (where particle horizons may be broken in specific directions), chaotic (‘mixmaster’) type behaviour [127] characterised by ‘billiard ball’ dynamics, and non-scalar singularities if the models are tilted. Dynamical systems methods can be used to show the dynamical behaviour of solutions and the relations of families of such models to each other [90]. If a cosmological model is generic, it should include Bianchi anisotropic modes as well as inhomogeneous modes, and may well show mixmaster behaviour [128].

4.6 Cosmological success and puzzles

Standard cosmology is a major application of GR showing how matter curves spacetime and spacetime determines the motion of matter and radiation. It is both a major success, showing how the dynamical nature of spacetime underlies the evolution of the universe itself, with this theory tested by a plethora of observations [10], and a puzzle, with three major elements of the standard model unknown (Dark matter, Dark energy, the Inflaton). While much of cosmological theory (the epoch since decoupling) follows from Newtonian gravitational theory (NGT), this is not true of the dynamics of the early universe, where pressure plays a key role in gravitational attraction: thus for example NGT cannot give the correct results for nucleosynthesis. The theory provides a coherent view of structure formation (with a few puzzles), and hence of how galaxies come into existence. The theory raises the issue that the universe not only evolves but (at least classically) had a beginning, whose dynamics lies outside the scope of standard physics because it lies outside of space and time. This is all discussed in depth in Chapter 4.

5 Gravitational Lensing and Dark Matter

The Schwarzschild solution predicts bending of light by massive objects: that is, gravitational lensing will occur. Indeed any mass concentration will differentially attract light rays; this is nowadays an important effect in astronomy and cosmology.

The bending of light by a gravitational field was predicted by Einstein in 1911 from the equivalence of a uniform gravitational field with an accelerated reference frame. In 1912 he derived an equation for gravitational lensing [129], well before he deduced the gravitational field equations. In 1915, he applied the gravitational field equations and found the deflection angle is twice the result obtained from the equivalence principle, the factor two arising because of the curvature of space. He predicted bending of light by the Sun in 1916, as famously verified by Eddington’s Expedition

in 1919, but he only published his pioneering paper on the bending of light by stars and galaxies in 1936 [130]. He stated there that the bending would not be observable in these cases because of the small angular scales involved, but recognised that lensing would cause fluctuations in the brightness of distant objects that might be detectable.

Gravitational lensing is now a key part of astronomy and cosmology [131, 132].

5.1 Calculating lensing

One can calculate deflection of light, and associated image displacement, distortion, and brightening, either through a weak field approximation, which will be valid for any mass distribution, or by determining geodesics in an exact solution, for example a spherically symmetric solution. They of course have to agree in the weak field approximation. Both show that for weak lensing, the angle of deflection of light caused by a spherical mass M is:

$$\hat{\alpha}(\xi) = \frac{4GM}{c^2} \frac{\xi}{|\xi|^2}$$

where ξ is the impact parameter, that is, the closest distance the light beam would reach from the centre of the lensing mass if there were no bending. Because the Schwarzschild radius of the Sun is 2.95 km and the solar radius is 6.96×10^5 km, a light ray grazing the limb of the Sun is deflected by an angle $(5.9/7.0) \times 10^{-5}$ radians = 1."7.

For more complex mass distributions, we represent the mass projected onto a mass sheet called the lens plane. Following Blandford and Narayan [133], a light ray from a source S at redshift z , is incident on a deflector or lens L at redshift z_d with impact parameter ξ relative to some fiducial lens center. Assuming the lens is thin compared to the total path length, its influence can be described by a deflection angle $\hat{\alpha}(\xi)$ (a two-vector) for the ray when it crosses the lens plane. The mass projected onto this plane is characterized by its surface mass density

$$\Sigma(\xi) = \int \rho(\xi, z) dz$$

where ξ is a two-dimensional vector in the lens plane. The deflection angle at position ξ is the sum of the deflections due to all the mass elements in the plane:

$$\hat{\alpha}(\xi) = \frac{4\pi G}{c^2} \int \frac{(\xi - \xi') \Sigma(\xi')}{|\xi - \xi'|^2} d^2 \xi'.$$

In the cosmological context, the intrinsic lensing angle $\hat{\alpha}(\theta)$ must be corrected to give the observed lensing angle α by using the angular diameter distances D_d , D_s , and D_{ds} between the source, deflector, and observer, which are affected by cosmological parameters. When the deflected ray reaches the observer, she sees the image of the source apparently at position θ on the sky. The true direction of the source, i.e. its position on the sky in the absence of the lens, is given by β . Now $\theta D_s = \beta D_s - \alpha D_{ds}$ where β is the angle from the source centre to the lensing element. Therefore, the positions of the source and the image are related through the lensing equation

$$\beta = \theta - \alpha(\theta)$$

where $\alpha(\theta) = \frac{D_{ds}}{D_s} \hat{\alpha}(D_d \theta)$. This light deflection leads to image distortion and amplification, characterised by the image magnification and shear. The shear is caused by the Weyl tensor the light encounters; the magnification is caused directly by the matter it encounters, and indirectly by the cumulative effect of the shear [91, 23, 5] (this follows from (1.5) with (1.8), and leads to (1.7)). The more mass (and the closer to the center of mass), the more the light is bent, and the more the image of a distant object is displaced, distorted, and perhaps magnified. These are the basic equations from which the cosmological applications follow.

5.2 Strong lensing

Lensing by galaxies can bend the light of a point background source by a large enough angle that it can be observed as several separate images. If the source, lensing object, and observer lie in a straight line, the source can appear as a ring around the lensing object (this is the case of Einstein rings). Misalignment will result in an arc segment instead. Lensing masses such as galaxy groups and clusters can result in the source being seen as many arcs around the lens. The observer may then see multiple distorted images of the same source, with time delays detectable between them if the source varies. The time delay between images is proportional to the difference in the absolute lengths of the light paths, which in turn is proportional to H_0 . The number and shape of the arcs depends on the relative positions of the source, lens, and the observer, as well as the gravitational well of the lensing object. The number and position of images is due to caustics in the light sheet that can be characterised as cusps, folds, etc. on using catastrophe theory [134]. Details are given in Chapter 3.

This effect enables detecting very distant galaxies that are otherwise unobservable. For example combining observations from the Hubble Space Telescope, Spitzer Space Telescope, and gravitational lensing by cluster Abell 2218, allowed discovery of the galaxy MACS0647-JD, that is roughly 13 billion light-years away. The galaxy appears 20 times larger and over three times brighter than typically lensed galaxies.

5.3 Weak lensing

Weak lensing results in image distortion, but the shear may be too small to be seen directly. Also apparent shear may be due to the galaxy's distinct shape, an angle of view that makes it appear elongated, or may be due to the telescope, the detector, or the atmosphere, so one cannot deduce weak lensing from images of a single object. However the faint distortions due to lensing of images of a set of galaxies can be worked out statistically, and the average shear due to lensing by some massive objects in front can be computed. Thus in the weak lensing case, measuring statistical distortion is the key to measuring the mass of the lensing object. Weak lensing surveys use this method to determine the intervening mass distribution. This is an important method in detecting dark matter [131]. Indeed the most important result from weak lensing concerns the proof of existence of collisionless dark matter in the 'bullet cluster' (see Chapter 3). An exciting recent application is detection of weak lensing in observations of CMB anisotropy patterns by the Planck satellite.

5.4 Microlensing

For point objects, it may happen that no distortion in shape can be seen but the amount of light received from a distant object changes in time, with a characteristic shape of the resulting light curve. The lensing objects may be stars in the Milky Way, with the source being stars in a remote galaxy, or a distant quasar. The method has been used to discover extrasolar planets, which is one of its most important applications.

5.5 Conclusion

Gravitational lensing was predicted very early on by Einstein and provided the first new observational evidence that vindicated general relativity. It is a confirmation of the curving of spacetime by matter and allows us to detect matter which has no other observational signature. It therefore plays a key role in the mapping of dark energy in the universe. It also acts as a lens allowing us to see far further than otherwise possible. It is thus a key tool in cosmology, discussed in the chapter 3.

6 Gravitational Waves

Einstein also predicted the existence of gravitational waves very early on [88]. However because of the coordinate freedom of general relativity, there was confusion as to whether these were real waves, or just coordinate waves. This was sorted out by the understanding, particularly due to Pirani, that the gravitational waves could be seen as Weyl tensor waves [22], which could carry away energy and momentum. They could therefore be indirectly observed by their effect on binary pulsar orbits, which can be measured to extremely high precision. Direct detection is much more difficult, but spectacular development in detector design promises that they may be detected in the next decades, with gravitational wave observatories having the potential to become an essential tool in precision cosmology. Crucial to this project are major developments in numerical relativity allowing us to predict the nature of waves expected to be emitted from binary blackhole mergers and other strong field sources.

6.1 Weak field formulation

Gravitational waves exist because GR is a relativistic theory of gravitation; unlike Newtonian theory, influences cannot be exerted instantaneously. Using a weak field approximation $g_{\mu\nu} = \eta_{\mu\nu} + h_{\mu\nu}$, $h_{\mu\nu} \ll 1$, and harmonic coordinates, Einstein predicted existence of waves in the metric tensor. But this may just be a wave in the coordinates! One can avoid this problem by using geometric variables, for example the 1+3 covariant representation of the Weyl tensor, whereby one obtains Maxwell like equations for the electric and magnetic parts of the Weyl tensor [114, 25, 26].

Nevertheless usual calculations use the weak field method of Einstein [88]. The perturbation h_{ab} is tracefree and transverse, so gravitational waves are transverse and, given their direction of propagation k , have two degrees of freedom (two polarisations) as represented by trace free 2-tensors orthogonal to k . That is, they are spin-2 fields. Defining $\bar{h}_{ab} \equiv h_{ab} - \frac{1}{2}\eta_{ab}h$ and choosing coordinates so that $\bar{h}^{ab}_{,b} = 0$, then on defining $z' = z - ct$, the two polarisation modes are $h_+(z')$ and $h_-(z')$, with weak field metric form

$$\begin{aligned} ds^2 &= -dt^2 + dx^2 + dy^2 + dz^2 + h_{\alpha\beta}(z')dx^\alpha dx^\beta \quad (h \ll 1), \\ h_{ab} &= \begin{pmatrix} 0 & 0 & 0 \\ 0 & h_+ & h_- \\ 0 & h_- & -h_+ \end{pmatrix}. \end{aligned}$$

One can get plane wave solutions of this form, characterised by their amplitude h , frequency f , wavelength λ , and speed c , related by the usual equation $c = \lambda f$. They can be linearly polarized, with quadrupole polarization components h_+ and h_\times in canonical coordinates, rotated by 45 degrees relative to each other. One can also have circularly polarized waves.

In the slow motion approximation for a weak metric perturbation for a source at distance r , the wave radiated by a local source is given by

$$h_{\mu\nu} = \frac{2G}{c^4 r} \frac{d^2 I_{\mu\nu}}{dt^2}$$

where $I_{\mu\nu}$ is the reduced quadrupole moment defined as

$$I_{\mu\nu} = \int \rho(\mathbf{r}) \left(x_\mu x_\nu - \frac{1}{3} \delta_{\mu\nu} r^2 \right) dV.$$

Hence gravitational waves are radiated by objects whose motion involves acceleration, provided that the motion is not perfectly spherically symmetric (the case of an expanding or contracting sphere). There are no spherical gravitational waves! An example is two gravitating objects that form a binary system. Seen from the plane of their orbits, the quadrupole term $I_{\mu\nu}$ will have non-zero second derivative.

6.2 Exact Gravitational waves

One can find exact gravitational wave solutions for cases with high symmetries.

6.2.1 Cylindrical gravitational waves

Einstein and Rosen [135] derived the exact solution for cylindrical gravitational waves. They state, “The rigorous solution for cylindrical gravitational waves is given. After encountering relationships which cast doubt on the existence of rigorous solutions for undulatory gravitational fields, we investigate rigorously the case of cylindrical gravitational waves. It turns out that rigorous solutions exist and that the problem reduces to the usual cylindrical waves in euclidean space.”

6.2.2 Plane gravitational waves

Plane gravitational waves are Petrov type N vacuum solutions that allow arbitrary information to be carried at the speed of light. They are exact solutions of the empty space field equations that can have high symmetries as studied by Ehlers and Kundt, and by Bondi, Pirani, and Robinson [136]. They have intriguing global properties due to the way they focus null geodesics [137]. One can find exact solutions for two colliding plane gravitational waves [138].

6.3 Asymptotic flatness and gravitational radiation

Gravitational waves can carry energy, momentum, and information, and it is useful to investigate this in general cases without symmetry. This can be done by asymptotic expansions in flat spacetimes, using multipole expansions clarified nicely by Thorne [14]. Following Trautman, outgoing radiation conditions have been formulated by Bondi, Sachs, Newman and Penrose, and others, leading to peeling-off theorems showing how successively different Petrov types occur at larger distances, and a ‘news function’ related to the derivative of shear is related to mass loss ([139, 19, 23]). Penrose showed how to express all this using his conformal representation of infinity [11]. Positive mass theorems aim to show that one cannot radiate so much mass away that the mass becomes negative [140, 141].

6.4 Emission

The linear perturbation formulae given above suffice for gravitational wave emission in weak field situations like the binary pulsar, and there is a large literature on analytic perturbations of black hole solutions [142] and the black hole perturbation approach to gravitational radiation [143, 144] as well as studies of gravitational waves from gravitational collapse [145] and from post-Newtonian sources and inspiralling compact binaries [146]. The Post-Newtonian (PN) approximation turned out to work even better than expected for inspiralling compact sources and it provides a very accurate and physical picture (including spins, eccentric orbits, tidal effects, etc). On the other hand key progress has come from major developments in numerical methods for examining non-linear relativity (NR) processes such as coalescence of two black holes, and associated numerical codes [147, 148, 149, 150]. Progress in this area has particularly been due to breakthroughs by Frans Pretorius.

These methods are complementary. The PN cannot describe the merger of two BHs, on the other hand NR will not be able to compute the inspiral of two BH or NS as does the PN, simply because of the prohibitive computing time needed to control 20,000 cycles before the coalescence, and the extreme accuracy of the PN at large separations. In LIGO/VIRGO detectors the PN plays a crucial role, both for detecting the signals on-line and for subsequent analysis and parameter estimation off-line. For sources like coalescing neutron stars, the templates are in fact completely based on the PN methods. Even for BH binaries with masses up to say 20 solar masses, the PN waveform

constitutes a large part of the templates. Idem for future supermassive BHs sources for LISA. The theoretical prediction from GR is a combination of PN for the inspiral and NR for the merger, both being accurately matched together.

Chapter 6 discusses the PN methods, and Chapter 7 discusses probing strong field gravity through numerical simulations.

6.5 Gravitational wave detection

As shown by Pirani, the effect of gravitational waves on local systems is via the (generalised) geodesic deviation equation [21, 22], which shows how the wave will tend to move particles transverse to the direction of motion in a quadrupole mode. Joseph Weber pioneered the effort to build gravitational detectors based on this effect, but it is enormously difficult technically because the strain is so small: typically of amplitude $h \simeq 10^{-20}$. Indirect detection via the effects of energy loss is easier.

6.5.1 Indirect detection: Binary pulsars

As noted above, emission requires anisotropic motion of a mass. This occurs in astronomical binary systems. If two masses m_1 and m_2 are in orbit around each other, separated by a distance r , the power radiated by this system is:

$$P = \frac{dE}{dt} = -\frac{32}{5} \frac{G^4}{c^5} \frac{(m_1 m_2)^2 (m_1 + m_2)}{r^5} \quad (21)$$

This energy loss will be reflected in a change in the orbital period, which is measurable in the case of binary pulsars because their precise pulse timing allows very accurate orbital tracking. Observations of binary pulsar decay rates by Hulse and Taylor confirmed this effect, and so confirmed the existence of gravitational radiation carrying energy away from the system [151, 152].

6.5.2 Indirect Detection: Inflation

Gravitational waves are expected to be emitted in the inflationary era in the very early universe and so CMB observations can provide evidence for their existence [153]. The relation between scalar contributions S to the quadrupole and tensor contributions T determines the amplitude (T/S). This is related to the tilt n_T by the key relation

$$n_T = -\frac{1}{7} \frac{T}{S} \quad (22)$$

which not only provides a consistency check of inflation, but it allows direct detection of gravity waves, as it relates the overall amplitude to the tilt [154]. The ratio T/S must be greater than 0.2 for a statistically significant detection of tensor perturbations. Gravitational waves will imprint as B-modes in the CMB anisotropy patterns, and so should be detectable by CMB polarisation measurements ([123, 86]). The value of the tensor to scalar ratio determined by observations such as those by Planck and BICEP2 strongly constrain models of inflation [155]. However foreground effects have to be very carefully controlled, and have undermined the original BICEP2 results.

6.5.3 Direct Detection by bars or interferometers

Ground-based direct detection is possible in principle via bar detectors or interferometers. Because of the very small size of the strain, this requires immense skill in technical development, discussed in Chapter 5; in particular it requires quantum non-demolition methods pioneered by Braginski. Gravitational-wave experiments with interferometers and with resonant masses can search for stochastic backgrounds of gravitational waves of cosmological origin. The sensitivity of these

detectors as a function of frequency has been carefully explored in relation to the expected astronomical sources, and this method has the prospect of opening up a new window on the universe because it will reach back to much earlier times than any other method [156, 157]. Direct detection of the inflationary gravitational wave background constrains inflationary parameters and complements CMB polarization measurements [158].

6.5.4 Pulsar timing arrays

Gravitational waves will affect the time a pulse takes to travel from a pulsar to the Earth. A pulsar timing array uses millisecond pulsars to search for effects of gravitational waves on measurements of pulse arrival times, giving delays of less than 10^{-6} seconds. Three pulsar timing array projects are searching for patterns of correlation and anti-correlation between signals from an array of pulsars that will signal the effects of gravitational waves.

6.6 Conclusion

The theory of gravitational waves extends the idea of transverse wave propagation from the spin-1 field of electromagnetism (Maxwell's theory) to the spin 2 field of gravitation. They are an essentially relativistic phenomenon: they cannot occur in Newtonian gravitational theory. Gravitational waves can carry energy and arbitrary information, and indeed convey information to us from the earliest history of the universe that we can access. They provide the ultimate limit of our possible access to knowledge about the early universe. Their direct detection is a formidable technological problem: the detectors being constructed are a triumph of theory realised in practice. Chapter 6 discusses sources of gravitational waves: theory and observations while Chapter 5 discusses current and future ground and space based laser interferometric gravitational wave observatories, pulsar timing arrays and the Einstein Telescope. It summarizes how these efforts will provide a brand new window on the universe.

7 Generalisations

Classical generalisations of general relativity include scalar tensor theories, higher derivative theories, theories with torsion, bimetric theories, unimodular theories, and higher dimensional theories. However if one demands only second order equations in four dimensions and with one spacetime metric, general relativity is the unique gravitational theory based in Riemannian geometry, as shown by Lovelock [159]. The theory was derived not because of experiment, but as the result of pure thought; but it has survived all experimental tests [40]: see Chapter 2. There is no observational or experimental reason to modify or abandon the field equations.

However there is a significant problem in terms of the relation of general relativity to quantum field theory calculations that predict existence of a vacuum energy density vastly greater than the observed value of the cosmological constant [160]. Possible solutions include either the existence of a multiverse combined with observational selection effects, or some form of unimodular gravity leading to the trace free form of the Einstein equations. In the latter case the exactly constant vacuum energy density does not gravitate, and this major problem is fully solved, with no change to all the results mentioned above in this chapter.

General relativity theory, and all its applications (most of which he pioneered), are yet another testament to Albert Einstein's extraordinary creativity and physical insight.

References

- [1] Stephani, H. *et al.* 2003. *Exact solutions of Einstein's field equations, Second edition*. Cambridge: Cambridge University Press. Corrected paperback reprint, 2009.
- [2] Ferreira, P. G. 2014. *The Perfect Theory: A Century of Geniuses and the Battle over General Relativity*. London: Little, Brown.
- [3] Einstein, A. 1915. *Sitzungsber. Preuss. Akad. Wiss. Berlin (Math. Phys.)*, **1915**, 844–847.
- [4] Misner, C. W., Thorne, K. S., and Wheeler, J. A. 1973. *Gravitation*. San Francisco: W. H. Freeman and Co.
- [5] Hawking, S. W., and Ellis, G. F. R. 1973. *The large scale structure of space-time*. Cambridge: Cambridge University Press.
- [6] Wald, R. M. 1984. *General relativity*. Chicago: University of Chicago Press.
- [7] Stephani, H. 1990. *General relativity: an introduction to the theory of the gravitational field (2nd edition)*. Cambridge: Cambridge University Press.
- [8] Synge, J. L., and Schild, A. 1949. *Tensor calculus*. Toronto: University of Toronto Press. Reprinted 1961.
- [9] Schouten, E. 1954. *Ricci calculus: an introduction to tensor analysis and its geometrical applications (2nd edition)*. Die Grundlehren der Mathematischen Wissenschaften, vol. X. Berlin: Springer.
- [10] Ellis, G. F. R., Maartens, R., and MacCallum, M. A. H. 2012. *Relativistic cosmology*. Cambridge: Cambridge University Press.
- [11] Penrose, R., and Rindler, W. 1984. *Spinors and space-time I: Two-spinor calculus and relativistic fields*. Cambridge: Cambridge University Press.
- [12] Ellis, G. F. R. 1967. *J. Math. Phys.* , **8**, 1171–1194.
- [13] Ellis, G. F. R., and MacCallum, M. A. H. 1969. *Com Math Phys*, **12**, 108–141.
- [14] Thorne, K. S. 1980. *Rev Mod Phys*, **52**, 299–340.
- [15] Challinor, A., and Lasenby, A. 1999. *Astrophys. J.* , **513**, 1–22.
- [16] Lewis, A., Challinor, A., and Lasenby, A. 2000. *Astrophys. J.* , **538**, 473–476.
- [17] Synge, J. L. 1937. *Proc. Lond. Math. Soc.*, **43**, 376. Reprinted as *Gen. Rel. Grav.* **41**, 2177 (2009).
- [18] Ehlers, J. 1961. *Akad. Wiss. Lit. Mainz, Abh. Math.-Nat. Kl.*, **11**. English translation by G. F. R. Ellis and P. K. S. Dunsby, in *Gen. Rel. Grav.* **25**, 1225–1266 (1993).
- [19] Sachs, R. K. 1962. *Proc. Roy. Soc. Lond. A*, **270**, 103–126.
- [20] Synge, J. L. 1934. *Ann. Math*, **35**, 705–713. Reprinted as *Gen. Rel. Grav.* **41**, 1206 (2009).
- [21] Pirani, F. A. E. 1956. *Acta. Phys. Polon.*, **15**, 389. Reprinted as *Gen. Rel. Grav.* **41** 1216 (2009).
- [22] Pirani, F. A. E. 1957. *Phys. Rev.*, **105**, 1089.

- [23] Newman, E. T., and Penrose, R. 1962. *J. Math. Phys.* , **3**, 566.
- [24] Raychaudhuri, A. K. 1955. *Phys. Rev.*, **98**, 1123–1126. Reprinted as *Gen. Rel. Grav.* **32**, 749 (2000).
- [25] Ellis, G. F. R. 1971. Relativistic cosmology. Pages 104–182 of: Sachs, R. K. (ed), *General relativity and cosmology*. Proceedings of the International School of Physics “Enrico Fermi”, vol. XLVII. New York and London: Academic Press. Reprinted as *Gen. Rel. Grav.* **41**, 581–660 (2009).
- [26] Maartens, R., and Bassett, B. A. C. C. 1998. *Class. Quantum Grav.* , **15**, 705–717.
- [27] Petrov, A. Z. 1954. *Scientific Proceedings of Kazan State University (named after V.I. Ulyanov-Lenin), Jubilee (1804-1954) Collection*, **114**, 55–69. Translation by J. Jezierski and M.A.H. MacCallum, with introduction by M.A.H. MacCallum, *Gen. Rel. Grav.* **32**, 1661–1685 (2000).
- [28] Penrose, R. 1960. *Ann. Phys. (USA)*, **10**, 171–201.
- [29] Israel, W. 1966. *Nuovo Cim. B*, **44**, 1–14. Erratum: *Nuovo Cim. B* **48**, 463 (1967).
- [30] Gödel, K. 1949. *Rev Mod Phys*, **21**, 447–450. Reprinted as *Gen. Rel. Grav.* **32**, 1409 (2000).
- [31] Penrose, R. 1964. Conformal treatment of infinity. Pages 565–584 of: DeWitt, B., and Dewitt, C. (eds), *Relativity, groups and topology*. New York: Gordon and Breach. Reprinted as *Gen. Rel. Grav.* **43**, 901–22 (2011).
- [32] Tipler, F. J., Clarke, C. J. S., and Ellis, G. F. R. 1980. Singularities and horizons: a review article. Page 97 of: Held, A. (ed), *General relativity and gravitation: one hundred years after the birth of Albert Einstein*, vol. 2. New York: Plenum.
- [33] Rindler, W. 1956. *Mon Not Roy Ast Soc*, **116**, 662. Reprinted as *Gen. Rel. Grav.* **34**, 133 (2002).
- [34] Stellmacher, K. 1938. *Math. Ann.*, **115**, 136–52. Reprinted as *Gen. Rel. Grav.* **42**, 1769–89 (2010).
- [35] Rendall, A. D. 2005. *Living Rev. Relativity*, **8**, 6.
- [36] Arnowitt, R., Deser, S., and Misner, C. W. 1962. The Dynamics of General Relativity. Pages 227–265 of: Witten, L. (ed), *Gravitation: An Introduction to Current Research*. New York and London: Wiley. Reprinted in *Gen. Rel. Grav.* **40**, 1997 (2008).
- [37] Penrose, R. 1965. *Phys. Rev. Lett.* , **14**, 579.
- [38] Hawking, S. W., and Penrose, R. 1970. *Proc. R. Soc. London A*, **314**, 529–548.
- [39] Curiel, E., and Bokulich, P. 2012. Singularities and Black Holes. In: Zalta, E. N. (ed), *The Stanford Encyclopedia of Philosophy (Fall 2012 Edition)*. Stanford: Stanford.
- [40] Will, C. M. 2006. *Living Rev. Relativity*, **9**.
- [41] Will, C. M. 1979. The confrontation between gravitational theory and experiment. In: Hawking, S., and Israel, W. (eds), *General Relativity: an Einstein centenary survey*. Cambridge: Cambridge University Press.
- [42] Fromholz, P., Poisson, E., and Clifford, C. M. 2014. *Amer. J. Phys.*, **82**, 295.
- [43] Schwarzschild, K. 1916. *Sitz. Preuss. Akad. Wiss.*, 189–196. Reprinted as *Gen. Rel. Grav.* **35**, 951 (2003).

- [44] Ashby, N. 2003. *Living Rev. Relativity*, **6**, 1.
- [45] Will, C. M. 2011. *Physics*, **4**, 43.
- [46] Breton, R. P. *et al.* 2008. *Science*, **321**, 104–107.
- [47] Reissner, H. 1916. *Ann. Phys. (Germany)*, **50**, 106–120.
- [48] Nordström, G. 1918. *Proc. Kon. Ned. Akad. Wet.*, **20**, 1238.
- [49] Kottler, F. 1918. *Ann. Phys. (Germany)*, **56**, 410–461.
- [50] Kerr, R. P. 1963. *J. Math. Mech.*, **12**, 33.
- [51] Kerr, R. P., and Schild, A. 1965. A New Class of Vacuum Solutions of the Einstein Field Equations. Pages 1–12 of: *Atti del Convegno sulla Relativita Generale: Problemi dell’ Energia e Onde Gravitazionali*. Firenze: Ed G. Barbera. Reprinted as *Gen. Rel. Grav.* **41**, 2485-99 (2009).
- [52] Abdelqader, M., and Lake, K. 2013. *Phys. Rev. D* , **88**, 064042.
- [53] Carter, B. 1968. *Commun. Math. Phys.*, **10**, 280–310.
- [54] Carter, B. 1973. Black Hole Equilibrium States, Part I Analytic and Geometric Properties of the Kerr Solutions. Pages 61–124 of: deWitt, C., and deWitt, B. (eds), *Black Holes - Les astres occlus*. New York: Gordon and Breach. Reprinted as *Gen. Rel. Grav.* **41**, 2874-938 (2009).
- [55] Eisenstaedt, J. 1982. *Arch. Hist. Exact Sci.*, **27**, 157–198.
- [56] Eisenstaedt, J. 1987. *Arch. Hist. Exact Sci.*, **37**, 275–357.
- [57] Eddington, A. S. 1924. *Nature*, **113**, 192.
- [58] Kruskal, M. D. 1960. *Phys. Rev.*, **119**, 1743–1745.
- [59] Boyer, R. H. 1969. *Proc. R. Soc. Lond. A*, **311**, 245–252.
- [60] Carter, B. 1968. *Phys. Rev.*, **174**, 1559–1571.
- [61] Boyer, R. H., and Lindquist, R. W. 1967. *J. Math. Phys.*, **8**, 265.
- [62] Lake, K., and Roeder, R. C. 1977. *Phys. Rev. D* , **15**, 3513–3519.
- [63] Tolman, R. 1934. *Proc. Nat. Acad. Sci.*, **20**, 169. Reprinted in *Gen. Rel. Grav.* , **29**, 935-943 (1997).
- [64] Bondi, H. 1947. *Mon NOT Roy Ast Soc*, **107**, 410. Reprinted as *Gen. Rel. Grav.* **31**, 1777-1781 (1999).
- [65] Krasinski, A. 2006. *Inhomogeneous cosmological models (2nd edition)*. Cambridge: Cambridge University Press.
- [66] Begelman, M., and Rees, M. J. 2010. *Gravity’s Fatal Attraction: Black Holes in the Universe*. Cambridge: Cambridge University Press.
- [67] Oppenheimer, J. R., and Snyder, H. 1939. *Phys Rev*, **56**, 455–459.
- [68] Israel, W. 1968. *Com math Phys*, **8**, 245–260.

- [69] Penrose, R. 1999. *J. Astrophys. Astr.*, **17**, 213–231.
- [70] Robinson, D. C. 1975. *Phys. Rev. Lett.* , **34**, 905–906.
- [71] Bardeen, J. M., Carter, B., and Hawking, S. W. 1973. *Com Math Phys*, **31**, 161–170.
- [72] Abramowicz, M. A., and Fragile, P. C. 2013. *Living Rev Relativity*, **16**, 1.
- [73] Rees, M. J. 1984. *Annual Review of Astronomy and Astrophysics*, **22**, 471–506.
- [74] Ferrarese, L., and Merritt, D. 2002. *Phys. World*, **15(6)**, 41–46.
- [75] Penrose, R. 1996. *J. Astrophys. Astr.*, **17**, 213–231.
- [76] Celotti, A., Miller, J. C., and Sciamia, D. W. 1999. *Class. Quantum Grav.* , **16**, A3–A21.
- [77] Schödel, R. *et al.* 2002. *Nature*, **419**, 694–696.
- [78] Melia, F. 2007. *The Galactic Supermassive Black Hole*. Princeton: Princeton University Press.
- [79] Einstein, A. 1917. *Sitzb. Preuss. Akad. Wiss.*, 142–152. English translation in ‘The Principle of Relativity’ by H.A. Lorentz, A. Einstein, H. Minkowski and H. Weyl (Dover: New York) 1923.
- [80] Friedmann, A. 1922. *Zeitschrift für Physik*, **10**, 377–386. Reprinted as *Gen. Rel. Grav.* **31**, 1991 (1999).
- [81] Friedmann, A. 1924. *Zeitschrift für Physik*, **21**, 326–332. Reprinted as *Gen. Rel. Grav.* **31**, 12 (1999).
- [82] Lemaître, G. 1931. *Nature*, **127**, 706.
- [83] Lemaître, G. 1933. *C. R. Acad. Sci. Paris*, **196**, 1085.
- [84] Ellis, G. F. R. 1990. Innovation, resistance and change: the transition to the expanding universe. Pages 97–114 of: Bertotti, B., Balbinot, R., Bergia, S., and Messina, A. (eds), *Modern Cosmology in Retrospect*. Cambridge: Cambridge University Press.
- [85] Robertson, H. P. 1933. *Rev. Mod. Phys.*, **5**, 62–90. Reprinted as *Gen. Rel. Grav.* **44**, 2115–2144 (2012).
- [86] Dodelson, S. 2003. *Modern Cosmology: Anisotropies and Inhomogeneities in the Universe*. Amsterdam: Academic Press.
- [87] Peter, P., and Uzan, J.-P. 2013. *Primordial Cosmology*. Oxford Graduate Texts. Oxford: Oxford University Press.
- [88] Einstein, A. 1918. *Sitzungsber. K. Preuss. Akad. Wiss.*, 154–167.
- [89] Ehlers, J., and Rindler, W. 1989. *Mon Not Roy Ast Soc*, **238**, 503–521.
- [90] Wainwright, J., and Ellis, G. F. R. 1997. *Dynamical systems in cosmology*. Cambridge: Cambridge University Press.
- [91] Kristian, J., and Sachs, R. K. 1966. *Astrophys. J.* , **143**, 379–399.
- [92] Etherington, I. M. H. 1933. *Phil. Mag.*, **15**, 761. Reprinted as *Gen. Rel. Grav.* **39**, 1055 (2007).
- [93] Sandage, A. 1961. *Astrophys. J.* , **133**, 355–392.

- [94] Ellis, G. F. R., and Rothman, T. 1993. *Amer. J. Phys.*, **61**, 883–893.
- [95] Wagoner, R. V., Fowler, W. A., and Hoyle, F. 1967. *Astrophys. J.* , **148**, 3–50.
- [96] Sunyaev, R. A., and Zeldovich, Y. B. 1970. *Astrophysics and Space Science*, **7**, 21–30.
- [97] Longair, M. 2013. *The Cosmic Century*. Cambridge: Cambridge University Press.
- [98] Doreshkevich, A., Zel’dovich, Y. B., and Novikov, I. D. 1967. *Soviet Astronomy AJ*, **11**, 233–239. Translated from *Astronomicheskii Zhurnal* **44**, 295–303.
- [99] Peebles, P. J. E. 1966. *Astrophys. J.* , **146**, 542–552.
- [100] Beringer, J. e. a. [Particle Data Group]. 2012. *Phys. Rev. D* , **86**, 010001.
- [101] Martin, J., Ringeval, C., and Vennin, V. 2013. *Encyclopaedia Inflationaris*. arXiv:arXiv:1303.3787.
- [102] Ellis, G. F. R., and Madsen, M. 1991. *Class. Quantum Grav.* , **8**, 667–676.
- [103] Lidsey, J. E. *et al.* 1997. *Rev. Mod. Phys.*, **69**, 373–410.
- [104] Peebles, P. J. E., and Yu, J. T. 1970. *Astrophys. J.* , **162**, 815.
- [105] Peebles, P. J. E. 1980. *The large-scale structure of the Universe*. Princeton: Princeton University Press.
- [106] Lemaître, G. 1933. *Ann. Soc. Sci. Bruxelles A*, **53**, 51. Translation by M. A. H. MacCallum in *Gen. Rel. Grav.* , **29**, 641–680 (1997).
- [107] Lemaître, G. 1949. *Rev Mod Phys*, **21**, 357.
- [108] Lemaître, G. 1958. *Pontifical Acad. Sci., Scripta Varia*, **16**, 475–488.
- [109] Lifshitz, E. M. 1946. *Acad. Sci. USSR. J. Phys.*, **10**, 116.
- [110] Sachs, R. K., and Wolfe, A. M. 1967. *Astrophys. J.* , **147**, 73. Reprinted as *Gen. Rel. Grav.* **39**, 1944 (2007).
- [111] Bardeen, J. M. 1980. *Phys. Rev. D* , **22**, 1882–1905.
- [112] Mukhanov, V. F., Feldman, H. A., and Brandenberger, R. H. 1992. *Phys Rep*, **215**, 203–333.
- [113] Kodama, H., and Sasaki, M. 1984. *Prog. Theor. Phys. Supp.*, **78**, 1–166.
- [114] Hawking, S. W. 1966. *Astrophys. J.* , **145**, 544–554.
- [115] Ellis, G. F. R., and Bruni, M. 1989. *Phys. Rev. D* , **40**, 1804–1818.
- [116] Bruni, M., Dunsby, P. K. S., and Ellis, G. F. R. 1992. *Astrophys. J.* , **395**, 34–53.
- [117] Mukhanov, V. F. 2005. *Physical Foundations of Cosmology*. Cambridge: Cambridge University Press.
- [118] Lahav, O., Lilje, P. B., Primack, J. R., and Rees, M. J. 1991. *Mon NOT Roy Ast Soc*, **251**, 128–136.
- [119] Sakharov, A. D. 1965. *Zh.E.T.F.*, **49**, 345–358. Translated as *Sov Phys JETP* bf 22, 241–249 (1966).

- [120] Sunyaev, R. A., and Zel'dovich, Y. B. 1970. *Astrophys Sp Sci*, **7**, 3.
- [121] Sunyaev, R. A., and Zeldovich, Y. B. 1980. *Annual review of astronomy and astrophysics*, **18**, 537–560.
- [122] Silk, J., and Wilson, M. L. 1979. *Astrophys. J.* , **228**, 641–646.
- [123] Bond, J. R., and Efstathiou, G. 1984. *Astrophys J*, **285**, L45–L48.
- [124] Efstathiou, G., Sutherland, W. J., and Maddox, S. J. 1990. *Nature*, **348**, 705–707.
- [125] Bonnor, W. B. 1956. *Z. Astrophys.*, **39**, 143. Reprinted as *Gen. Rel. Grav.* **30** 1113–1132 (1998).
- [126] Mustapha, N., Hellaby, C. W., and Ellis, G. F. R. 1999. *mon Not Roy Ast Soc*, **292**, 817–830.
- [127] Misner, C. W. 1969. *Phys. Rev. Lett.* , **22**, 1071–1074.
- [128] Lifshitz, E. M., and Khalatnikov, I. M. 1964. *Sov. Phys. Usp.*, **6**, 495–522.
- [129] Renn, J., Sauer, T., and Stachel, J. 1997. *Science*, **275**, 184–186.
- [130] Einstein, A. 1936. *Science*, **84**, 506–7.
- [131] Schneider, P., Ehlers, J., and Falco, E. E. 1992. *Gravitational lenses*. New York: Springer-Verlag.
- [132] Wambsganss, J. 2001. *Living Rev. Relativity*.
- [133] Blandford, R. D., and Narayan, R. 1992. *Ann. Rev. Astron. Astrophys.*, **30**, 311–358.
- [134] Perlick, V. 2004. *Living Rev. Relativity*.
- [135] Einstein, A., and Rosen, N. J. 1937. *J. Franklin Inst.*, **223**, 43.
- [136] Bondi, H., Pirani, F. A. E., and Robinson, I. 1959. *Proc. Roy. Soc. Lond. A*, **251**, 519–533.
- [137] Penrose, R. 1965. *Rev. Mod. Phys.*, **37**, 215.
- [138] Szekeres, P. 1972. *J. Math. Phys.*, **13**, 286–294.
- [139] Bondi, H., van der Burg, M. G. J., and Metzner, A. W. K. 1962. *Proc. Roy. Soc. London A*, **269**, 21.
- [140] Schoen, R., and Yau, S.-T. 1979. *Comm Math Phys*, **65**, 45–76.
- [141] Witten, E. 1981. *Com Math Phys*, **80**, 381–402.
- [142] Teukolsky, S. A. 1973. *Astrophys. J.* , **185**, 635–648.
- [143] Sasaki, M., and Tagoshi, H. 2003. *Living Rev. Relativity*, **6**, 6.
- [144] Kokkotas, K. D., and Schmidt, B. 1999. *Living Rev. Relativity*, **2**, 2.
- [145] Fryer, C. L., and New, K. C. B. 2011. *Living Rev. Relativity*, **14**, 1.
- [146] Blanchet, L. 2006. *Living Rev. Relativity*, **9**, 4.
- [147] Owen, R. *et al.* 2011. *Phys. Rev. Lett.* , **106**, 151101.
- [148] Nichols, D. A. *et al.* 2011. *Phys. Rev. D* , **84**, 124014.

- [149] Zhang, F. *et al.* 2012. *Phys. Rev. D* , **86**, 084049.
- [150] Nichols, D. A. *et al.* 2012. *Phys. Rev. D* , **86**, 104028.
- [151] Taylor, J. H., Fowler, L. A., and McCulloch, P. M. 1979. *Nature*, **277**, 437–440.
- [152] Taylor, J. H., and Weisberg, J. M. 1989. *Astrophys. J.* , **345**, 434–450.
- [153] Turner, M. S., White, M. J., and Lidsey, J. E. 1993. *Phys. Rev. D* , **48**, 4613–4622.
- [154] Turner, M. S. 1996. *Phys. Rev. D* , **55**, 435–439.
- [155] Martin, J., Ringeval, C., Trota, R., and Vennin, V., 2014. [arXiv:1405.7272](https://arxiv.org/abs/1405.7272).
- [156] Krauss, L. M., Dodelson, S., and Meyer, S. 2010. *Science*, **328**, 989–992.
- [157] Sathyaprakash, B. S., and Schutz, B. F. 2009. *Living Rev. Relativity*, **12**, 2.
- [158] Kuroyanagi, S., Gordon, C., Silk, J., and Sugiyama, N. 2010. *Phys. Rev. D* , **81**, 083524.
- [159] Lovelock, D. 1971. *J. Math. Phys.* , **12**, 498.
- [160] Weinberg, S. 1989. *Rev. Mod. Phys.*, **61**, 1–23.